Novel anti-inflammatory agent 3-[(dodecylthiocarbonyl)-methyl]-glutarimide ameliorates murine models of inflammatory bowel disease

Nobuki Ichikawa[1], Kenichiro Yamashita[2*], Tohru Funakoshi[1], Shin Ichihara[3], Moto Fukai[1], Masaomi Ogura[1], Nozomi Kobayashi[1], Masaaki Zaitsu[1], Tadashi Yoshida[1], Susumu Shibasaki[1], Yasuyuki Koshizuka[1], Yusuke Tsunetoshi[1], Masanori Sato[1], Takahiro Einama[1], Michitaka Ozaki[1], Kazuo Umezawa[4], Tomomi Suzuki[1], Satoru Todo[1,2*]

Departments of [1]Gastroenterological Surgery I and [2]Transplant Surgery, Graduate School of Medicine, Hokkaido University, N-15, W-7, Kita-ku, Sapporo 060-8638, Japan

[3]Department of Surgical Pathology, Sapporo-Kosei General Hospital l, N-3, E-8-5, Chuo-ku, Sapporo 060-0033, Japan

[4]Department of Molecular Target Medicine Screening, Aichi Medical University, Yazakokarimata 1-1, Nagakute 480-1195, Japan

[*]Both authors contributed equally as senior authors.

Corresponding authors:

Kenichiro Yamashita, M.D., Ph.D. and Satoru Todo, M.D.

Department of Transplant Surgery, Graduate School of Medicine, Hokkaido University, N-15, W-7, Kita-ku, Sapporo 060-8638, Japan

Phone: +81-11-706-7765; Fax: +81-11-706-7064

E-mail: kenchan@med.hokudai.ac.jp (K. Yamashita); s-todo@st-mary-med.or.jp (S. Todo)

Abstract

Objective and design To examine the effect of 3-[(dodecylthiocarbonyl)-methyl]-glutarimide (DTCM-G), a novel anti-inflammatory agent that inhibits lipopolysaccharide (LPS) -activation of RAW264.7 macrophages, on murine models of colitis and RAW264.7 cells.

Materials and Methods Colitis was induced by rectally infusing trinitrobenzenesulfonic acid (TNBS) (1.5 mg in 50% ethanol) in BALB/c mice or orally administering 3% dextran sulfate sodium (DSS) for 5 days in C57BL/6 mice. The severity of colitis was assessed after intraperitoneally injecting DTCM-G (40 mg/kg). The anti-inflammatory properties of DTCM-G and its mechanisms were investigated in LPS-stimulated RAW264.7 cells.

Results DTCM-G significantly ameliorated TNBS-induced colitis, according to the body weight loss, disease activity index, colonic obstruction, macroscopic colonic inflammation score, mucosal myeloperoxidase activity, and histopathology. Immunohistochemistry and isolated lamina propria mononuclear cells showed significantly reduced colonic $F4/80^+$ and $CD11b^+$ macrophage infiltration. DTCM-G significantly suppressed tumor necrosis factor (TNF)-α and interleukin (IL)-6 messenger RNA expression in the colon, and attenuated DSS-induced colitis, according to the disease activity index and histopathology. In RAW264.7 cells, DTCM-G suppressed LPS-induced TNF-α/IL-6 production and enhanced glycogen synthase kinase-3β phosphorylation.

Conclusions DTCM-G attenuated murine experimental colitis by inhibiting macrophage infiltration and inflammatory cytokine expression. Thus, DTCM-G may be a promising treatment for inflammatory bowel disease.

Keywords: Inflammatory bowel disease, 3-[(dodecylthiocarbonyl)-methyl]-glutarimide, trinitrobenzenesulfonic acid, dextran sulfate sodium, colitis, macrophage

Introduction

Human inflammatory bowel disease (IBD) is clinically characterized by two subtypes: Crohn's disease and ulcerative colitis. This idiopathic, inflammatory disease of the digestive tract occurs worldwide. IBD is a chronic, progressive, and destructive disease that causes irreversible structural bowel damage and results in loss of intestinal function; it frequently requires bowel resection [1]. Although the etiology is partially unknown, emerging evidence suggests that the disease develops in genetically predisposed individuals through a dysregulated response of the mucosal immune system to environmental factors such as intraluminal bacterial antigens [2]. Attempts to prevent and reduce mucosal inflammation pharmacologically with aminosalicylates, corticosteroids, immunosuppressive compounds, and/or antibiotics have failed to achieve and maintain remission in approximately 30% of patients. In addition, these agents have many undesirable side effects such as impaired glucose tolerance, adrenal suppression, increased infection risk, hepatitis, pancreatitis, and bone marrow suppression. Therefore, novel anti-inflammatory drugs for treating IBD are warranted [1, 3].

Macrophages play a critical role in the pathogenesis of IBD. Patients with an active IBD status have elevated numbers of activated monocytes/macrophages in their peripheral blood [4]. In active IBD mucosa, monocyte-derived activated macrophages [5] along with chemokine gradients from the inflamed mucosa [6] mediate immune responses by producing inflammatory cytokines, including tumor necrosis factor (TNF)-α and interleukin (IL)-6 [7], chemokines such as IL-8 and monocyte chemotactic protein (MCP)-1 [6], and matrix metalloproteinases [8]. In IBD patients, inhibitors of macrophage activation have shown therapeutic potential and clinical benefits. RDP58, an anti-inflammatory peptide that inhibits activation of the MyD88-IRAK-TRAF6

protein complex upstream of the mitogen-activated protein kinase (MAPK) signaling pathway, reduces simple clinical colitis activity index values as well as sigmoidoscopy and histology scores in patients with mild-to-moderate ulcerative colitis [9]. Semapimod is a small molecule (about 890 Da) that blocks MAPK phosphorylation and ATP binding, and it improves the Crohn's Disease Activity Index in patients with moderate-to-severe Crohn's disease [10, 11].

Previously, we synthesized a low molecular-weight compound, dehydroxymethylepoxyquinomycin, from the antibiotic epoxyquinomycin C [12], which inhibits nuclear factor (NF)-κB activation [12] and ameliorates dextran sulfate sodium (DSS)-induced colitis in mice [13]. During the search for potent anti-inflammatory agents, a number of analogs were synthesized, and we synthesized 3-[(dodecylthiocarbonyl)-methyl]-glutarimide (DTCM-G; 355 Da) from the antibiotic 9-methylstreptimidone [14]. DTCM-G inhibited the lipopolysaccharide (LPS)-mediated activation of the activator protein-1 but not NF-κB, and it suppressed the production of inducible nitric oxide synthase/cyclooxygenase 2 in RAW264.7 cells [14]. In addition, we showed that DTCM-G inhibits cell cycle progression and proliferation of activated murine primary T-cells via the suppression of the mammalian target of rapamycin signaling pathway in vitro, and it prolongs allograft survival in heart transplant recipient mice [15]. Therefore, in the current study, we examined the anti-inflammatory effects of DTCM-G in IBD using two murine colitis models and investigated the underlying mechanism.

Materials and methods

Cells and the Cell Culture

The murine macrophage-like cell line RAW264.7 was obtained from the Riken Cell Bank (Tsukuba, Japan). The cells were cultured in Dulbecco's modified Eagle's medium (DMEM; Sigma-Aldrich, Tokyo, Japan) containing 2 mM L-glutamine, 100 U/mL penicillin, 100 μg/mL streptomycin, 10% fetal calf serum, and 50 μM 2-mercaptoethanol, and they were maintained at 37°C in an incubator with 5% CO_2 and 100% humidity.

DTCM-G

Aliquots of 100 mg/mL DTCM-G in dimethylsulfoxide (DMSO) were stored at -80°C until use. For in vivo experiments, the stock solution was diluted in 0.5% carboxymethyl cellulose (CMC) solution (final DMSO concentration, 4%), whereas for in vitro experiments, the stock was diluted in 0.04% DMSO.

Mice

Male BALB/c mice (8–10 weeks old; weight, 24–26 g) and C57BL/6 mice (8–10 weeks old; weight, 22–24 g) were obtained from Japan SLC Inc. (Shizuoka, Japan). The Hokkaido University Institutional Animal Care Committee approved the study protocol and the guidelines of the animal care policy were followed.

Colitis Induction and Treatment Protocols

Trinitrobenzenesulfonic acid colitis

Twelve-hour fasted BALB/c mice were anesthetized using isoflurane, and a 3.5 French catheter was inserted

into the colon 4 cm proximal to the anus. Trinitrobenzenesulfonic (TNBS) (1.5 mg in 150 µL 50% ethanol; Sigma-Aldrich) was administered in the lumen using a 1 mL syringe. Then the mice were maintained in a vertical position for 30 s to ensure proper TNBS distribution within the colon. After colitis induction, 40 mg/kg DTCM-G was administered by an intraperitoneal injection twice daily during days 0–4. The control animals were treated with vehicle injections (0.5% CMC containing 4% DMSO). The experiments were repeated three to five times with six animals/group/experiment.

DSS colitis

Drinking water containing 3% DSS (36–50 kDa; MP Biomedicals Inc., Tokyo, Japan) was provided ad libitum to the C57BL/6 mice for 5 days. Thereafter, the mice received regular water for 5 days. In the treatment group, either 20 or 40 mg/kg DTCM-G was injected intraperitoneally twice daily from days 0–10 after initial DSS administration. The control mice received vehicle injections (0.5% CMC containing 4% DMSO). The experiments were repeated thrice with six animals/group/experiment.

Colitis Assessment

TNBS colitis

The mice's body weight, blood in the stool, and stool consistency were monitored daily. Blood in the stool was assessed using Hemoccult slides (Shionogi and Co Ltd., Osaka, Japan). The animals were euthanized on day 4, and the presence of colonic obstruction was evaluated. The mice's colons were collected without the cecum, and we measured the colonic length and evaluated it for macro/microscopic damage. The severity of the colitis was

assessed according to the weight loss, disease activity index (DAI), colonic obstruction, macroscopic score, colonic length, myeloperoxidase activity, and histological damage. The DAI was calculated by grading the following parameters on a scale of 0–4: change in body weight (0: ≤1%, 1: 1–5%, 2: 6–10%, 3: 11–20%, and 4: >20%), blood in stool (0: negative, 1–3: Hemoccult positive, and 4: gross bleeding), and stool consistency (0: normal, 1: soft stools, 2: loose stools, 3: muddy stools, and 4: diarrhea) [16]. Macroscopic scores were graded in a blinded fashion on a scale of 0–10 as follows: 0, normal appearance; 1, focal hyperemia without ulcers; 2, ulceration without hyperemia or bowel wall thickening; 3, ulceration with inflammation at one site; 4, ulceration or inflammation at ≥2 sites; 5, major sites of damage extending 1 cm along the length of the colon; and 6–10, the score increased by 1 for each additional centimeter involved in the damage extending ≥2 cm along the length of the colon [17].

DSS colitis

The mice's body weight, blood in the stool, and stool consistency were monitored daily. The animals were euthanized on day 10, and their large intestines were collected without the cecum. The severity of the colitis was assessed according to the DAI and histological damage.

Histopathological Examination

TNBS colitis

A colon specimen was excised precisely 1 cm from the terminal ileum, fixed in 10% phosphate-buffered formalin, embedded in paraffin, sectioned, and stained with hematoxylin and eosin. Histological scoring of the

tissues was performed from three experiments using six mice per group by a skilled pathologist in a blinded manner. Histological damage was categorized into five distinct groups, and each were graded as follows: grade 0, no sign of inflammation; grade 1, very low -level leukocyte infiltration; grade 2, low -level leukocyte infiltration; grade 3, high -level leukocyte infiltration, high vascular density, and thickened colonic wall; and grade 4, transmural leukocyte infiltration, goblet cell loss, high vascular density, and thickened colonic wall [18]. To assess the infiltrated neutrophils, the colon sections were obtained on day 0 (before colitis induction) and day 2, and on day 4 they were evaluated histologically. Neutrophils were counted from the images (final magnification, ×200) of the two most severely inflamed fields from four animals in each group.

DSS colitis

Specimens of the entire colon without the cecum were fixed in formalin, embedded in paraffin, sectioned, and stained with hematoxylin and eosin. Histological scoring of the tissues was performed from three experiments using six mice per group by a skilled pathologist in a blinded manner. The severity of the colitis was assessed according to the scoring system described by Dieleman et al. [19]. The grading index was as follows: inflammation severity (0: none, 1: mild, 2: moderate, and 3: severe), inflammation extent (0: none; 1: mucosa, 2: mucosa and submucosa, and 3: transmural), crypt damage (0: none, 1: one-third of the basal tissue is damaged, 2: two-thirds of the basal tissue is damaged, 3: only the surface epithelium is intact, and 4: the entire crypt and epithelium is lost), and the percentage involved in the ulcer or erosion (1: <1%, 2: 1–15%, 3: 16–30%, 4: 31–45%, and 5: 46–100%). The sum of the first three scores (severity, extent, and crypt damage) was multiplied by the percentage involvement score to obtain the final value for comparison.

Immunohistochemical Analysis

Colon infiltration by mononuclear cells was evaluated by immunohistochemistry. Tissue samples were freshly frozen in the Tissue-Tek® O.C.T.™ compound (Sakura Finetechnical, Tokyo, Japan). Five-μm cryosections fixed in acetone were pretreated with 1% H_2O_2-phosphate buffered saline (PBS) and were incubated with rat anti-mouse CD4 (GK1.5; Santa Cruz Biotechnology Inc., Tokyo, Japan), CD8 (MCA609EL; Serotec Ltd., Oxford, United Kingdom), or F4/80 monoclonal antibodies (MC497R; Serotec Ltd.) at 4°C overnight. Then the sections were washed with PBS and incubated with normal mouse serum and biotinylated anti-rat IgG (Vector Lab, Inc., Burlingame, CA) in PBS for 30 min. The immunolabeled cells were visualized with diaminobenzidine (Dako Ltd., Tokyo, Japan). The sections were lightly counterstained with hematoxylin. Cells positive for F4/80, CD4, or CD8 were counted (except for cells in the colonic lymphoid follicles) for a high power field (magnification, ×200) within the three most severely inflamed fields using four mice per group. Colon infiltration by neutrophils was also evaluated by immunohistochemistry. Five-μm cryosections fixed in paraformaldehyde were pretreated with 1% H_2O_2-methanol and were incubated with polyclonal rabbit anti-human myeloperoxidase (Dako, Glostrup, Denmark) at room temperature for 60 min. Then the sections were washed with PBS and incubated with anti-rabbit EnVision (Dako) for 30 min. The immunolabeled cells were visualized with diaminobenzidine (Dako Ltd.). The sections were lightly counterstained with hematoxylin. Cells positive for myeloperoxidase were counted for a high power field (magnification, ×200) within the two most severely inflamed fields using four mice per group.

Myeloperoxidase Assay

The myeloperoxidase activity in colonic tissues, a proxy for neutrophil activity, was determined as previously reported [20]. Briefly, the colon tissues were homogenized in 50-mmol/L phosphate buffer containing 0.5% hexadecyltrimethyl ammonium bromide. After centrifugation at 20,000 ×g, supernatants were spectrophotometrically assayed for myeloperoxidase activity by a chromogenic reaction with o-dianisidine dihydrochloride and H_2O_2. Data are presented as the optical density at 460-nm/mg tissue from three experiments using four mice per group.

Phenotypic Analysis of Lamina Propria Mononuclear Cells

The lamina propria mononuclear cells (LPMCs) were isolated from freshly obtained colon specimens from TNBS-colitis mice as previously described [21]. The colon specimens without the cecum were opened longitudinally, rinsed in PBS, and treated with 1 mM of ethylenediaminetetraacetic acid in calcium- and magnesium-free Hank buffered saline solution for 15 min to remove the epithelium. Then the tissues were digested with 1 mg/mL of collagenase D (Roche Diagnostics, Indianapolis, IN) for 20 min in a shaking incubator at 37°C. Next, the released cells were layered on a 40–75% Percoll™ PLUS gradient (GE Healthcare UK Ltd., Little Chalfont, UK) and were centrifuged at 600 ×g for 20 min to obtain a leukocyte-enriched population on the surface of the 75% interface. The LPMCs were stained by fluorescein isothiocyanate-CD4 (L3T4; Becton Dickinson and Co., Franklin Lakes, NJ), peridinin chlorophyll-CD8 (53-6.7; Becton Dickinson),

and phycoerythrin-CD11b (M1/70; Becton Dickinson) antibodies as well as their corresponding isotype-matched fluorescein isothiocyanate, peridinin chlorophyll, or phycoerythrin-conjugated rat immunoglobulins. Additionally, they were analyzed by flow cytometry using FACSCalibur™ (Becton Dickinson). The data were analyzed using FlowJo software (Tree Star, Inc., Ashland, OR). For phenotypic analysis, the LPMCs from the DTCM-G treatment group were compared with LPMCs from the vehicle-injected and naïve groups (age-matched healthy non-colitis mice; n = 4 animals in all groups).

3-[4,5-dimethylthiazol-2-yl]-2,5-diphenyltetrazoliumbromide Assay

The RAW264.7 cells were serum-starved in DMEM/0.5% fetal calf serum overnight. After 2 h of incubation in DMEM/10% fetal calf serum, the cells (1×10^4 cells/mL, 100 μL/well) were seeded into 96-well plates. The cells were pretreated with 0–20 μg/mL DTCM-G for 2 h followed by 1 μg/mL of LPS for another 8 h. Then 0.5 mg/mL of 3-[4,5-dimethylthiazol-2-yl]-2,5-diphenyltetrazoliumbromide (MTT) was added to each well, and the cells were incubated for 4 h at 37°C under 5% CO_2. Subsequently, the culture supernatants were replaced with 100 μL of DMSO to dissolve the formazan crystals, which were formed by mitochondrial succinic dehydrogenase metabolism of the MTT substrate. Absorbance at 570 nm was measured in triplicate wells from three independent experiments using a microplate reader (Varioskan® Flash; Thermo Fisher Scientific Inc., Waltham, MA).

Measuring the Cytokine Release

The RAW264.7 cells (1×10^4 cells/well) were serum-starved overnight in 96-well plates. After preincubation with serum-containing media, the cells were treated with either 7.5 μg/mL of DTCM-G or the vehicle for 2 h and were then stimulated with 1 μg/mL of LPS. The supernatant was collected after 24 h of LPS stimulation, and the IL-6 and TNF-α levels were measured using an enzyme-linked immunosorbent assay kit (R&D Systems, Minneapolis, MN) in triplicate wells from three independent experiments.

Real-Time Reverse Transcription Polymerase Chain Reaction

Colon tissues without the cecum were snap-frozen in liquid nitrogen and stored at -80°C. Total ribonucleic acid (RNA) was extracted using Trizol® (Invitrogen Life Technologies Japan Ltd., Tokyo, Japan). One μg total messenger (m)-RNA was reverse transcribed at 37°C using the Omniscript™ Reverse Transcription Kit (Qiagen K.K., Tokyo, Japan) with an oligo (dT) 20 primer (Toyobo Co Ltd., Osaka, Japan) and Protector RNase inhibitor (Roche Diagnostics K.K., Tokyo, Japan). Real-time polymerase chain reaction (PCR) was performed using a QuantiTect SYBR Green PCR Kit (Qiagen) and the LightCycler® Carousel-Based System (Roche Diagnostics). The primers (Life Technologies Japan Ltd., Tokyo, Japan) were designed using Primer3 software (web version 0.4.0; Howard Hughes Medical Institute, Chevy Chase, MD, USA) using sequences published in the National Center for Biotechnology Information database. The cycling conditions were as follows: 40 cycles at 94°C for 15 s, 60°C for 20 s, and 72°C for 30 s. The specificity of the PCR products was confirmed by melting curves, and the data were analyzed using Roche LightCycler® data analysis software and plasmid deoxyribonucleic acid (DNA) standards. The mRNA levels were normalized to

glyceraldehyde 3-phosphate dehydrogenase (GAPDH) levels and were quantified relative to the untreated mice (n = 8 mice/group). The PCR primers for murine GAPDH were 5-TACACTGAGGACCAGGTTGT and 5-CTGTAGCCGTATTCATTGTC; interferon (IFN)-γ, 5- GCGTCATTGAATCACACCTG and 5-TGAGCTCATTGAATGCTTGG; IL-10, 5- GGTTGCCAAGCCTTATCGGA and 5-ACCTGCTCCACTGCCTTGCT; MCP-1, 5- TCCCAATGAGTAGGCTGGAG and 5-TCTGGACCCATTCCTTCTTG; TNF-α, 5- ACCCTCACACTCAGATCATC and 5-GAGTAGACGAGTAGACAAGGTACAACCC; IL-1β, 5- GGATGAGGACATGAGCACCT and 5-AGCTCATATGGGTCCGACAG; and IL-6, 5- GAAAGCCAGAGTCCTTCAGAG and 5-CCACTCCTTCTGTGACTCC.

Western Blot Analysis

Following overnight starvation and preincubation with serum-containing media, the RAW264.7 cells were treated with 7.5 μg/mL of DTCM-G for 2 h and then stimulated with 1 μg/mL of LPS for 0, 5, 15, or 45 min. The medium was removed at different time points, and the cells were snap-frozen at -80°C until use. For protein extraction, the cells were collected in 200 μL of an ice-cold radioimmunoprecipitation assay buffer (Takara Bio Inc., Shiga, Japan) containing 25 mM of Tris-HCl pH 7.6, 150 mM of NaCl, 1% NP-40, 1% sodium deoxycholate, 0.1% SDS, and Halt™ Protease/Phosphatase Inhibitor Cocktail (Thermo Fisher Scientific), sonicated for 1–2 s, incubated on ice for 5 min, and centrifuged at 600 ×g for 10 min. The protein concentration was determined using the bicinchoninic acid protein assay kit (Thermo Fisher Scientific). The samples were

stored at -80°C until use. Equivalent amounts of proteins (40 μg) were fractionated on 10% Tris-glycine gels (Mini-PROTEAN® TGX™; Bio-Rad Laboratories, Inc., Tokyo, Japan) by sodium dodecyl sulfate-polyacrylamide gel electrophoresis and transferred to polyvinylidene difluoride membranes. Non-specific binding was blocked by incubation with 3% bovine serum albumin in 0.1% Tween 20/Tris-buffered saline. Then the membranes were incubated overnight at 4°C with primary antibodies against PDK1, phospho-PDK1 (serine 241; C49H2), AKT, phospho-AKT (serine 473; D9E), phospho-AKT (threonine 308; C31E5E), c-Raf, phospho-c-Raf (serine 259), $p70^{S6K}$, phospho-$p70^{S6K}$ (threonine 421/serine 424), GSK3β (27C10), or phospho-GSK-3β (serine 9; D85E2; all from Cell Signaling Technology Japan K.K., Tokyo, Japan). Cytoplasmic GAPDH (14C10; Cell Signaling Technology) was used as a control for overall protein loading. The membranes were washed with 0.1% Tween 20/Tris-buffered saline, incubated with horseradish peroxidase-conjugated secondary antibody (Cell Signaling Technology), rewashed, and incubated with the Super Signal™ West Dura extended duration chemiluminescent substrate (Thermo Fisher Scientific) for 5 min, after which they were exposed to film (ChemiDoc™ MP System, Bio-Rad Laboratories). The experiments were repeated three times in an independent manner.

Statistical Analysis

Data are expressed as the mean ± standard error of the mean or mean ± standard deviation (for LPMC counts) of the indicated numbers of samples. Statistical analysis was performed using StatView software, version 5.0 (SAS Institute, Inc., Cary, NC, USA). Body weight changes, the DAI, macroscopic and

histopathological scores, colon length, the rate of small bowel obstruction, cell counts and mRNA levels for TNBS-induced colitis, histopathological scores for DSS-induced colitis, and immunoblot protein band densities were analyzed using Student's t-test. Data from the myeloperoxidase assay, LPMC count, MTT assay, and cytokine measurements were compared using one-way analysis of variance with Bonferroni correction. In contrast, body weight changes and the DAI were compared using repeated measures analysis of variance with Bonferroni correction. Differences were considered statistically significant if the P value was <0.05.

Results

DTCM-G Inhibits Colon Inflammation in TNBS-induced colitis

To investigate the therapeutic potential of DTCM-G in IBD, we used a murine model of TNBS-induced colitis. Intra-colonic TNBS administration caused severe illness characterized by weight loss and diarrhea. Twice-daily intraperitoneal treatment with 40 mg/kg of DTCM-G significantly affected weight loss on day 4 ($p = 0.04$ vs. control, Fig. 1A) and improved the DAI on days 2–4 ($p < 0.05$, Fig. 1B). In the control mice, the colon wall was thickened, and the rate of colon obstruction was $66.7 \pm 11.8\%$ on day 4. In contrast, treatment with DTCM-G significantly abrogated colon obstruction to $6.7 \pm 6.1\%$ on day 4 ($p < 0.01$, Fig. 1C). Furthermore, DTCM-G improved the macroscopic disease score, which was indicated by the remission of bowel-wall thickening, hyperemia, and colon ulceration (Fig. 1D). Moreover, DTCM-G treatment prevented TNBS-induced shortening of the colon by day 4 (Fig. 1E).

DTCM-G Ameliorates TNBS-induced Colitis

The severity of colon inflammation was further evaluated by histopathological examination and the myeloperoxidase assay. In the vehicle-only control animals, the histopathology of colons obtained on day 4 showed marked wall thickening with a severe inflammatory cellular infiltrate in the lamina propria and the muscular and serosal layers (Fig. 2A). Conversely, colon tissues from DTCM-G-treated animals had minor subepithelial edema and mild inflammatory cell infiltration of the mucosa and submucosa (Fig. 2B). DTCM-G treatment significantly improved the pathological scores in terms of the neutrophil infiltration, loss of goblet cells, vascular density, and thickening of the colon wall (Fig. 2C). To assess the inflammation severity of the colon, infiltrated neutrophils were quantified in colon tissue sections on day 0 (before colitis induction), day 2, and day 4. Neutrophil counts significantly increased on day 2 ($p < 0.01$ vs. naïve, non-colitis mice) and day 4 ($p < 0.01$ vs. naïve mice) in the control mice, and they were significantly reduced in the DTCM-G treatment group ($p=0.01$ vs. control, Fig. 2E). In addition, myeloperoxidase activity in the colon tissues was markedly lower in the DTCM-G treated group than in the controls on day 4 (Fig. 2F).

DTCM-G Reduces the Number of Macrophages and $CD4^+$ Lymphocytes in LPMCs

We analyzed infiltrated LPMCs during TNBS-induced colitis development. Immunohistochemical analysis detected infiltration of $F4/80^+$ cells into the lamina propria and muscular and subserosal layers of the control animals' colons, whereas $CD4^+$ and $CD8^+$ cells were present in the submucosal lesions. $F4/80^+$ ($p < 0.01$ vs. naïve) and $CD4^+$ ($p = 0.02$ vs. naïve) cell counts peaked in the control animals' colons on day 2, whereas

$CD8^+$ cell numbers did not increase. DTCM-G significantly reduced $F4/80^+$ ($p = 0.02$ vs. controls) and $CD4^+$ ($p < 0.01$ vs. control) cell infiltration on day 2 (Fig. 3A–C). To confirm the DTCM-G-mediated inhibition of LPMC infiltration, we isolated LPMCs from freshly obtained TNBS-induced colons. We obtained $2.9 \pm 1.9 \times 10^6$ LPMCs from the control mice, but only $0.7 \pm 0.4 \times 10^6$ cells ($p < 0.01$) from the naïve non-colitis mice. DTCM-G treatment significantly reduced the infiltrated LPMC count to $1.1 \pm 0.5 \times 10^6$ cells versus the controls ($p = 0.01$). Flow cytometric analysis showed that the majority of LPMCs in inflamed colons were $CD11b^+$ cells, and the percentages of $CD11b^+$ cells relative to total LPMCs in the naïve, control, and treated mice were 1.7%, 69.1%, and 59.6%, respectively (Fig. 3E). The number of infiltrating $CD11b^+$ cells increased to $18.0 \pm 10.8 \times 10^5$ cells in the control mice versus only $0.1 \pm 0.1 \times 10^6$ cells in the naïve mice ($p < 0.01$), and DTCM-G treatment significantly reduced $CD11b^+$ cellular infiltrates to $5.5 \pm 2.1 \times 10^5$ cells ($p = 0.01$ vs. control, Fig. 3D). The number of $CD4^+$ cells also increased from $4.8 \pm 2.3 \times 10^4$ cells in the naïve mice to $7.4 \pm 4.3 \times 10^4$ cells in the control TNBS-colitis mouse colons. DTCM-G treatment also reduced the colitis-induced increase of $CD4^+$ cells to $3.1 \pm 1.8 \times 10^4$ cells; however, the difference was not statistically significant (Fig. 3F). The percentages of $CD4^+$ cells relative to total lymphocytes of the lamina propria in the naïve, control, and treated mice were 12.7%, 17.9%, and 19.2%, respectively. The difference was not statistically significant (Fig. 3G). The number of $CD8^+$ cells in the colon was not altered by TNBS administration (Fig. 3H). The difference of the percentages of $CD8^+$ cells among three groups was not significant either (Fig. 3I).

DTCM-G Suppresses Inflammatory Cytokine/Chemokine Gene Expression in the Colon Mucosa

To examine whether the DTCM-G -mediated suppression of TNBS-induced colitis was associated with decreased inflammatory mediator expression, the mRNAs from day 2 colon specimens were analyzed. At this time, LPMC infiltration was at its peak. Expression of the genes encoding IFN-γ, IL-10, TNF-α, IL-1β, IL-6, and MCP-1 was significantly increased in colons from TNBS-treated animals versus naïve animal colons (Fig. 4). In fact, the expression of the genes encoding TNF-α, IL-6, and MCP-1 was significantly downregulated by DTCM-G treatment (Fig. 4).

DTCM-G Ameliorates DSS-mediated Colitis

Next, we examined the effect of DTCM-G in the DSS-induced colitis model. Following oral DSS administration, the mice exhibited severe bloody diarrhea accompanied by extensive weight loss. Vehicle-only treatment did not improve these symptoms. In contrast, DTCM-G treatment inhibited body weight loss on days 7–10 and improved the DAI on days 6–10 in a dose-dependent manner (Fig. 5A–B). Furthermore, histopathology indicated that DTCM-G ameliorated DSS-induced colitis. Colon sections on day 10 showed that vehicle-treated animals had severe colitis with colon wall thickening, ulceration, crypt damage, and pronounced inflammatory infiltrates in the lamina propria and muscular and serosal layers (Fig. 5C). Conversely, colon specimens from DTCM-G-treated animals exhibited only mild subepithelial edema with minimal inflammatory infiltrates in the mucosa and submucosa (Fig. 5D). The total pathological scores for colitis significantly improved ($p = 0.01$, Fig. 5E), which manifested as an improvement in all the criteria, including inflammation

severity and depth, crypt damage, and epithelial regeneration (data not shown).

DTCM-G Suppresses Inflammatory Cytokine Production in Activated RAW264.7 Macrophages

Since DTCM-G ameliorated colonic inflammation and suppressed macrophage infiltration in mouse models of colitis, we further examined the effects of DTCM-G in the RAW264.7 murine macrophage-like cell line. First, we assessed the direct cellular cytotoxicity of DTCM-G using the MTT assay. At concentrations ≤10 μg/mL, DTCM-G did not significantly alter the number of viable cells (Fig. 6A). However, at a concentration of 0–10 μg/mL, DTCM-G reduced IL-6 and TNF-α production from LPS-stimulated RAW264.7 cells in a concentration-dependent manner (Fig. 6B).

DTCM-G Promotes GSK-3β Phosphorylation

To elucidate the underlying mechanism by which DTCM-G suppresses inflammatory cytokine production in LPS-stimulated RAW264.7 cells, the proteins were analyzed by Western blotting using total and phospho-specific antibodies against PDK1, AKT, c-Raf, $p70^{S6K}$, and GSK-3β. Phosphorylation of AKT (serine 473) and GSK-3β was enhanced after LPS stimulation. DTCM-G inhibited LPS-induced AKT phosphorylation, whereas DTCM-G further upregulated LPS-induced GSK-3β phosphorylation over time (Fig. 7). Following LPS stimulation, $p70^{S6K}$, c-Raf, and PDK1 phosphorylation was also upregulated in the RAW264.7 cells, but this effect was not altered by DTCM-G treatment (Fig. 7).

Discussion

We examined the potential of DTCM-G as a candidate therapeutic drug for IBD by using two experimental murine colitis models. In the TNBS-induced colitis model, which mimics Crohn's disease to a certain extent [22], DTCM-G administration significantly ameliorated colon injury according to the body weight loss, stool consistency and blood score, colon obstruction, macroscopic colon inflammation score, myeloperoxidase activity, and colon histopathology. This effect was reproducible in a murine DSS-induced colitis model that mimics human ulcerative colitis [23], wherein DTCM-G significantly ameliorated colon injury according to the body weight loss, DAI, and colon histopathology.

Using the TNBS-induced colitis model, we attempted to elucidate the underlying mechanism of DTCM-G-mediated amelioration of colonic injury. In the preliminary study, we confirmed the clinical course of our TNBS colitis model. The clinical symptom in our model recovered gradually after day 4, as assessed by the DAI and body weight change (data not shown). Therefore, we examined a 4-day course in the TNBS colitis model with or without DTCM-G treatment. Following TNBS induction, the both macrophages and $CD4^+$ cells transiently increased and peaked along with the clinical course, as previously reported [24,25]. The neutrophils increased thereafter, as also shown previously by Palman et al. [26].

The TNBS model was originally established as a colitis model involving oligoclonal expansion and activation of $CD4^+$ T lymphocytes in response to TNBS-haptenized self-antigens [27]. Previously, we demonstrated that DTCM-G suppressed the proliferation and IFN-γ production of activated murine primary T cells, and that DTCM-G prolongs cardiac allograft survival in mice [15]. Therefore, we initially hypothesized

that DTCM-G ameliorated TNBS colitis by inhibiting $CD4^+$ T lymphocytes. However, when isolated colon LPMCs were examined, DTCM-G did not inhibit concanavalin A-mediated proliferation or change constituent $CD4^+$ T lymphocyte phenotypes in terms of T-bet and CD25/Foxp3 expression in treated versus control animals (data not shown). These results mean that DTCM-G did not suppress the proliferation of $CD4^+$ T lymphocyte nor did it induce differentiation to Th1/Treg cells in colon LPMCs. However, it is certain that DTCM-G treatment suppressed $CD4^+$ lymphocyte infiltration of the colon and reduced IFN-γ mRNA expression in the colon tissues of TNBS colitis. The *ex vivo* experiment of LPMCs did not necessarily reflect the *in vivo* colon inflammation and DTCM-G suppressed proliferation of IFN-γ producing T cells in colon tissue. Another possible mechanism for how DTCM-G reduced the number of infiltrated $CD4^+$ T lymphocyte and IFN-γ mRNA expression in the colon is that DTCM-G inhibited chemokine (i.e., MCP-1; Fig. 4E) expression and lessened the migration of leukocytes, including $CD4^+$ T lymphocyte, as was shown by Khan et al.'s study that DNBS colitis in MCP-1-deficient mice develop less severe colitis, and the infiltration of T cells and IFN-γ production were suppressed [28].

In addition to $CD4^+$ T cells, TNBS-induced colitis was characterized by lamina propria infiltration of monocytes/macrophages and neutrophils that peaked on days 2 and 4, respectively. Previously, it was demonstrated that macrophages heavily infiltrate the colon following TNBS-induced colitis [26], and that the removal of macrophages using either anti-CD1lb or anti-CD18 antibodies prevented TNBS -colitis in mice [29, 30]. In addition to cellular infiltrates, the mRNA expression of macrophage-derived inflammatory cytokines such as TNF-α, IL-6, and MCP-1 [31, 32] was elevated in the TNBS-injured colon on day 2. These findings

indicate that DTCM-G inhibits TNBS-induced inflammatory responses in the colon by inhibiting macrophage activation. Therefore, we focused specifically on the inhibitory effect of DTCM-G on macrophages, and elucidated the underlying mechanisms using the murine macrophage-like cell line, RAW264.7. DTCM-G suppressed IL-6 and TNF-α production in LPS-stimulated RAW264.7 cells. These findings are in line with previous data by Takeiri et al. [14], which indicated that DTCM-G inhibited inducible nitric oxide synthase and cyclooxygenase 2 expression in a similar macrophage cell line.

An earlier study by Takeiri et al. demonstrated that the inactivation of RAW264.7 cells by DTCM-G was mediated by the suppression of the activator protein-1 cascade, not the MAPK signaling pathway, and activation of NF-κB, cAMP response element-binding protein, and CCAAT/enhancer binding protein β [14]. We previously demonstrated that DTCM-G inhibited $p70^{S6K}$ phosphorylation and c-Jun DNA binding in primary murine T cells following cell activation by anti-CD3/anti-CD28 monoclonal antibodies [15]. Since $p70^{S6K}$ is a downstream effector molecule of the AKT signaling pathway [33], we examined whether DTCM-G affected AKT and $p70^{S6K}$ activation in LPS-stimulated RAW264.7 cells. Although DTCM-G suppressed AKT phosphorylation at serine 473, it did not inhibit $p70^{S6K}$ or c-Raf phosphorylation. However, we could not detect the protein of phosphorylated AKT at Thr 308 in any of the experimental groups (data not shown). In contrast, DTCM-G significantly promoted the phosphorylation of GSK-3β in LPS-stimulated RAW264.7 cells. Since phosphorylation-mediated GSK-3β inactivation resulted in anti-inflammatory reactions [34, 35], we believe that GSK-3β suppression in macrophages is a likely mechanism of DTCM-G-mediated inhibition of inflammatory

colon injury. Indeed, inhibiting GSK-3β via phosphoinositide 3-kinase knockdown prevented self-induced colitis [36]. Furthermore, the GSK-3β inhibitor LiCl/SB216763 ameliorated DSS-induced colitis in mice [37].

No apparent DTCM-G-related toxicity was noted in colitis-induced mice when DTCM-G was administered at a daily dose of <80 mg/kg, according to the body weight loss and stool conditions. Detailed studies confirming its safety and efficacy in higher animal species are necessary before considering DTCM-G for clinical applications. Comparison with known compounds or studies on oral administration will further determine its potential as a drug. Finally, we conclude that DTCM-G attenuates experimental colitis in mice by inhibiting macrophage activation and infiltration. Thus, DTCM-G appears to be a potential candidate for treating IBDs.

Acknowledgements

This study was supported in part by funding from the Promotion of Fundamental Studies in Health Sciences initiative of the National Institute of Biomedical Innovation and a Grant-in-Aid for Scientific Research (C) from the Japan Society for the Promotion of Science.

Conflict of Interest

The authors declare no conflicts of interest.

Compliance with Ethical Standards

All applicable international, national, and/or institutional guidelines for the care and use of animals were followed. All the procedures performed in studies involving animals were in accordance with the ethical standards of the institution or practice at which the studies were conducted.

References

1. Sandborn WJ. Current directions in IBD therapy: what goals are feasible with biological modifiers? Gastroenterology. 2008;135:1442–7.

2. Baumgart DC, Carding SR. Inflammatory bowel disease: cause and immunobiology. Lancet. 2007;369:1627–40.

3. Baumgart DC, Sandborn WJ. Inflammatory bowel disease: clinical aspects and established and evolving therapies. Lancet. 2007;369:1641–57.

4. Hanai H, Iida T, Takeuchi K, Watanabe F, Yamada M, Kikuyama M, et al. Adsorptive depletion of elevated proinflammatory CD14+CD16+DR++ monocytes in patients with inflammatory bowel disease. Am J Gastroenterol. 2008;103:1210–6.

5. Grimm MC, Pullman WE, Bennett GM, Sullivan PJ, Pavli P, Doe WF. Direct evidence of monocyte recruitment to inflammatory bowel disease mucosa. J Gastroenterol Hepatol. 1995;10:387–95.

6. Zimmerman NP, Vongsa RA, Wendt MK, Dwinell MB. Chemokines and chemokine receptors in mucosal homeostasis at the intestinal epithelial barrier in inflammatory bowel disease. Inflamm Bowel Dis. 2008;14:1000–11.

7. Reimund JM, Wittersheim C, Dumont S, Muller CD, Baumann R, Poindron P, et al. Mucosal inflammatory cytokine production by intestinal biopsies in patients with ulcerative colitis and Crohn's disease. J Clin Immunol. 1996;16:144–50.

8. von Lampe B, Barthel B, Coupland SE, Riecken EO, Rosewicz S. Differential expression of matrix

metalloproteinases and their tissue inhibitors in colon mucosa of patients with inflammatory bowel disease. Gut. 2000;47:63–73.

9. Travis S, Yap LM, Hawkey C, Warren B, Lazarov M, Fong T, et al. RDP58 is a novel and potentially effective oral therapy for ulcerative colitis. Inflamm Bowel Dis. 2005;11:713–9.

10. Hommes D, van den Blink B, Plasse T, Bartelsman J, Xu C, Macpherson B, et al. Inhibition of stress-activated MAP kinases induces clinical improvement in moderate to severe Crohn's disease. Gastroenterology. 2002;122:7–14.

11. Dotan I, Rachmilewitz D, Schreiber S, Eliakim R, van der Woude CJ, Kornbluth A, et al. A randomised placebo-controlled multicentre trial of intravenous semapimod HCl for moderate to severe Crohn’s disease. Gut. 2010;59:760–6.

12. Matsumoto N, Ariga A, To-e S, Nakamura H, Agata N, Hirano S, et al. Synthesis of NF-kappaB activation inhibitors derived from epoxyquinomicin C. Bioorg Med Chem Lett. 2000;10:865–9.

13. Funakoshi T, Yamashita K, Ichikawa N, Fukai M, Suzuki T, Goto R, et al. A novel NF-κB inhibitor, dehydroxymethylepoxyquinomicin, ameliorates inflammatory colonic injury in mice. J Crohns Colitis. 2012;6:215–25.

14. Takeiri M, Tachibana M, Kaneda A, Ito A, Ishikawa Y, Nishiyama S, et al. Inhibition of macrophage activation and suppression of graft rejection by DTCM-glutarimide, a novel piperidine derived from the antibiotic 9-methylstreptimidone. Inflamm Res. 2011;60:879–88.

15. Shibasaki S, Yamashita K, Goto R, Wakayama K, Tsunetoshi Y, Zaitsu M, et al. Immunosuppressive

effects of DTCM-G, a novel inhibitor of the mTOR downstream signaling pathway. Transplantation. 2013;95:542–50.

16. Cooper HS, Murthy SN, Shah RS, Sedergran DJ. Clinicopathologic study of dextran sulfate sodium experimental murine colitis. Lab Invest. 1993;69:238–49.

17. Wallace JL, Keenan CM, Gale D, Shoupe TS. Exacerbation of experimental colitis by nonsteroidal anti-inflammatory drugs is not related to elevated leukotriene B4 synthesis. Gastroenterology. 1992;102:18–27.

18. Neurath MF, Fuss I, Kelsall BL, Stüber E, Strober W. Antibodies to interleukin 12 abrogate established experimental colitis in mice. J Exp Med. 1995;182:1281–90.

19. Dieleman LA, Palmen MJ, Akol H, Bloemena E, Peña AS, Meuwissen SG, et al. Chronic experimental colitis induced by dextransulphate sodium (DSS) is characterized by Th1 and Th2 cytokines. Clin Exp Immunol. 1998;114:385–91.

20. Bradley PP, Priebat DA, Christensen RD, Rothstein G. Measurement of cutaneous Inflammation: Estimation of neutrophil content with an enzyme marker. J Invest Dermatol. 1982;78:206–9.

21. Dohi T, Fujihashi K, Rennert PD, Iwatani K, Kiyono H, McGhee JR. Hapten-induced colitis is associated with colonic patch hypertrophy and T helper cell 2-type responses. J Exp Med. 1999;189:1169–80.

22. te Velde AA, Verstege MI, Hommes DW. Critical appraisal of the current practice in murine TNBS-induced colitis. Inflamm Bowel Dis. 2006;12:995–9.

23. Okayasu I, Hatakeyama S, Yamada M, Ohkusa T, Inagaki Y, Nakaya R. A novel method in the induction of

reliable experimental acute and chronic ulcerative colitis in mice. Gastroenterology. 1990;98:694–702.

24. Hollenbach E, Vieth M, Roessner A, Neumann M, Malfertheiner P, Naumann M. Inhibition of RICK/nuclear factor-kappaB and p38 signaling attenuates the inflammatory response in a murine model of Crohn disease. J Biol Chem. 2005;280:14981–8.

25. Pereira-Fantini PM, Judd LM, Kalantzis A, Peterson A, Ernst M, Heath JK, et al. A33 antigen-deficient mice have defective colonic mucosal repair. Inflamm Bowel Dis.2010;16:604-12.

26. Palmen MJ, Dieleman LA, van der Ende MB, Uyterlinde A, Peña AS, Meuwissen SG, et al. Non-lymphoid and lymphoid cells in acute, chronic and relapsing experimental colitis. Clin Exp Immunol. 1995;99:226–32.

27. Morris GP, Beck PL, Herridge MS, Depew WT, Szewczuk MR, Wallace JL. Hapten-induced model of chronic inflammation and ulceration in the rat colon. Gastroenterology. 1989;96:795–803.

28. Khan WI, Motomura Y, Wang H, El-Sharkawy RT, Verdu EF, Verma-Gandhu M, et al. Critical role of MCP-1 in the pathogenesis of experimental colitis in the context of immune and enterochromaffin cells. Am J Physiol Gastrointest Liver Physiol. 2006;291:G803–11.

29. Kanai T, Watanabe M, Okazawa A, Sato T, Yamazaki M, Okamoto S, et al. Macrophage-derived IL-18-mediated intestinal inflammation in the murine model of Crohn's disease. Gastroenterology. 2001;121:875–88.

30. Palmen MJ, Dijkstra CD, van der Ende MB, Peña AS, van Rees EP. Anti-CD1lb/CD18 antibodies reduce inflammation in acute colitis in rats. Clin Exp Immunol. 1995;101:351–56.

31. Woywodt A, Ludwig D, Neustock P, Kruse A, Schwarting K, Jantschek G, et al. Mucosal cytokine expression, cellular markers and adhesion molecules in inflammatory bowel disease. Eur J Gastroenterol Hepatol. 1999;11:267–76.

32. Neurath MF, Fuss I, Pasparakis M, Alexopoulou L, Haralambous S, Meyer zum Büschenfelde KH, et al. Predominant pathogenic role of tumor necrosis factor in experimental colitis in mice. Eur J Immunol. 1997;27:1743–50.

33. Salh B, Wagey R, Marotta A, Tao JS, Pelech S. Activation of phosphatidylinositol 3-kinase, protein kinase B, and p70 S6 kinases in lipopolysaccharide-stimulated Raw 264.7 cells: differential effects of rapamycin, Ly294002, and wortmannin on nitric oxide production. J Immunol. 1998;161:6947–54.

34. Martin M, Rehani K, Jope RS, Michalek SM. Toll-like receptor-mediated cytokine production is differentially regulated by glycogen synthase kinase 3. Nat Immunol. 2005;6:777–84.

35. Steinbrecher KA, Wilson W 3rd, Cogswell PC, Baldwin AS. Glycogen synthase kinase 3 functions to specify gene-specific, NF-κB-dependent transcription. Mol Cell Biol. 2005;25:8444–55.

36. Uno JK, Rao KN, Matsuoka K, Sheikh SZ, Kobayashi T, Li F, et al. Altered macrophage function contributes to colitis in mice defective in the phosphoinositide-3 kinase subunit p110δ. Gastroenterology. 2010;139:1642–53.

37. Hofmann C, Dunger N, Schölmerich J, Falk W, Obermeier F. Glycogen synthase kinase 3-β: a master regulator of toll-like receptor-mediated chronic intestinal inflammation. Inflamm Bowel Dis. 2010;16:1850–58.

Figure Legends

Fig. 1 3-[(dodecylthiocarbonyl)-methyl]-glutarimide (DTCM-G) inhibits colon inflammation in trinitrobenzenesulfonic acid (TNBS)-induced colitis

TNBS (1.5 mg/mouse; 150 μL containing 50% ethanol) was rectally administered to BALB/c mice. DTCM-G (40 mg/kg) was administered intraperitoneally every 12 h for 4 days following the TNBS enema. Body weight (A) and disease activity index (B) were assessed daily. The severity of colitis was assessed by colonic obstruction (C), the macroscopic score (D), and colon length (E) on day 4. Results represent the mean ± standard error of the mean from five experiments with six mice per group (* $p < 0.05$ and <0.0167 vs. the control mice).

Fig. 2 3-[(dodecylthiocarbonyl)-methyl]-glutarimide (DTCM-G) improves the colon pathology in trinitrobenzenesulfonic acid (TNBS)-induced murine colitis

Paraffin-embedded colon sections from day 4 were stained with hematoxylin and eosin and were evaluated histologically. Representative photographs of the treatment with control vehicle injections (A) and twice daily 40 mg/kg DTCM-G injections (B) are shown (original magnification, ×40). (C)The severity of the colonic injury was assessed by the pathological scores. Results represent the mean ± standard error of the mean from three experiments using six mice per group (* $p < 0.05$ vs. the vehicle-injected control mice). (D,E) Colon cryosections on days 0 (before colitis induction), 2, and 4 were immunostained with myeloperoxidase, and the neutrophils were counted from photographs (original magnification, ×200) of the two most severely inflamed

fields or mice colons. (D) Representative photographs are shown (original magnification above, ×40; original magnification below, ×200). (E) Results represent the mean ± standard error of the mean (n = 4 animals in each group; * $p < 0.05$ vs. the control mice). (F) Myeloperoxidase activity/mg colon tissue was measured using a chromogenic enzymatic assay from fresh colon (day 4). Data are presented as an optical density at 460 nm/mg of tissue. Results represent the mean ± standard error of the mean from three experiments using four mice per group (¶ < 0.0167 vs. the control mice).

Fig. 3 3-[(dodecylthiocarbonyl)-methyl]-glutarimide (DTCM-G) reduces the number of macrophages and $CD4^+$ lymphocytes in lamina propria mononuclear cells (LPMCs) from trinitrobenzenesulfonic acid (TNBS)-induced colitis tissue

(A–C) Mononuclear cell infiltration of the lamina propria (LP) was evaluated by immunohistochemistry. Representative photographs of each result are also shown (original magnification above, ×40; original magnification below, ×200). Colon cryosections were immunostained for (A) F4/80, (B) CD4, or (C) CD8, and the positive cells were counted (cells in the colonic lymphoid follicles are omitted). Each result represents the mean ± standard error of the mean from three most severely inflamed fields using four mice per group (* $p < 0.05$ vs. the vehicle-only treated mice). (D–I) LPMCs were isolated from fresh colon specimens (day 2) of TNBS-induced colitis mice, and they were immunostained with phycoerythrin-CD11b, fluorescein isothiocyanate-CD4, and peridinin chlorophyll-CD8 antibodies (F). Flow cytometric data were analyzed using FlowJo software (Treestar, Inc.). The number of the $CD11b^+$ cells (D), $CD4^+$ cells (F), $CD8^+$ cells (H) from the

DTCM-G treatment group (n = 4) were compared with those from the vehicle control and naïve groups. Results represent the mean ± standard deviation from four mice ($p < 0.0167$ vs. the vehicle-only control mice). Representative FACS profiles of $CD11b^+$ cells (E), $CD4^+$ cells (G), $CD8^+$ cells (I) are also shown (the isotype control is represented by a dotted line. A positive event was defined as 5% of events of isotype control.)

Fig. 4 3-[(dodecylthiocarbonyl)-methyl]-glutarimide (DTCM-G) alters cytokine and chemokine gene expression in the colon mucosa during the early stage of trinitrobenzenesulfonic acid (TNBS)-induced murine colitis

Cytokine/chemokine messenger ribonucleic acid (mRNA) expression in freshly obtained colon tissue on day 2 of TNBS colitis was measured using real-time polymerase chain reaction. The expression of interferon (IFN)-γ (A), tumor necrosis factor-α (B), interleukin (IL)-1β (C), IL-6 (D), monocyte chemoattractant protein-1 (E), and IL-10 (F) genes are shown. The mRNA levels are represented as fold-increase versus naïve (no colitis) mice. All results were normalized to tissue glyceraldehyde 3-phosphate dehydrogenase expression and were determined in duplicate. Data represent the mean ± standard error of the mean (n = 8 mice/group; * $p < 0.05$ vs. the vehicle-injected control mice).

Fig. 5 3-[(dodecylthiocarbonyl)-methyl]-glutarimide (DTCM-G) ameliorates dextran sulfate sodium (DSS) colitis

DSS (3% final concentration) was added to the drinking water that was provided ad libitum to C57BL/6 mice for 5 days. DTCM-G at 20 mg/kg (Δ) or 40 mg/kg (□), or vehicle-only (○) was administered intraperitoneally

every 12 h on days 0–10. The severity of colitis was assessed by changes in the body weight (BW; A) and disease activity index (DAI; B). Results represent the mean ± standard error of the mean from three experiments with six mice/group (*, ‡ $p < 0.0167$ vs. the vehicle control treatment groups, † $p < 0.0167$ vs. both vehicle control treatment groups and the 20 mg/kg DTCM-G treatment groups). Paraffin-embedded sections obtained on day 10 were stained with hematoxylin and eosin and were evaluated histologically. Representative photomicrographs of colon sections following treatment with the vehicle only (C) and 40 mg/kg DTCM-G (D) are shown (original magnification, ×40). (E) The severity of colon injury was assessed by pathological scoring. Results represent the mean ± standard error of the mean of three independent experiments consisting of six mice/group/experiment (* $p < 0.05$ vs. the vehicle-only control mice).

Fig. 6 3-[(dodecylthiocarbonyl)-methyl]-glutarimide (DTCM-G) suppresses inflammatory cytokine production in lipopolysaccharide (LPS)-stimulated RAW264.7 macrophages

(A) After pre-incubation with serum-containing media, RAW264.7 cells were treated with 0–20 μg/mL DTCM-G for 2 h and were then stimulated with 1 μg/mL LPS for 8 h. Next, 3-[4,5-dimethylthiazol-2-yl]-2,5-diphenyltetrazoliumbromide (MTT) solution was added for 4 h, and absorbance at 570 nm was measured using a microplate reader (* $p < 0.0018$ vs. the dimethyl sulfoxide [DMSO]-only treated cells). (B) After preincubation with serum-containing media, the cells were treated with 7.5 μg/mL DTCM-G for 2 h and were then stimulated with 1 μg/mL of LPS for 24 h. Supernatants were collected and assayed for interleukin-6 and tumor necrosis factor-α levels by enzyme-linked immunosorbent

assays. All results were examined in triplicate wells and were represented as a mean ± standard error of the mean from three independent experiments (* $p < 0.0023$ vs. the DMSO-only treated cells).

Fig. 7 3-[(dodecylthiocarbonyl)-methyl]-glutarimide (DTCM-G) enhances glycogen synthase kinase (GSK)-3β phosphorylation in lipopolysaccharide (LPS)-stimulated RAW264.7 cells

(A) RAW264.7 cells were treated with either 0.04% dimethyl sulfoxide (vehicle) or 7.5 μg/mL DTCM-G for 2 h prior to 0–45 min of 1 μg/mL of LPS stimulation. The cellular proteins were analyzed by immunoblotting with total and phospho-specific antibodies against PDK1, AKT, c-Raf, $p70^{S6K}$, and GSK-3β. Glyceraldehyde 3-phosphate dehydrogenase (GAPDH) expression was used as a loading control. Representative immunoblots of three independent experiments are shown. (B) The intensity of each band was densitometrically quantified for analysis. All results were normalized to GAPDH expression levels and were represented as the mean ± standard error of the mean of three independent experiments. The bar in each figure expresses a one-fold increase in the average of the naïve specimens. (* $p < 0.05$ vs. the DMSO-only controls). (C) Schematic of the PI3K-Akt-GSK3 signaling pathway. DTCM-G promotes phosphorylation-mediated GSK-3β inactivation.

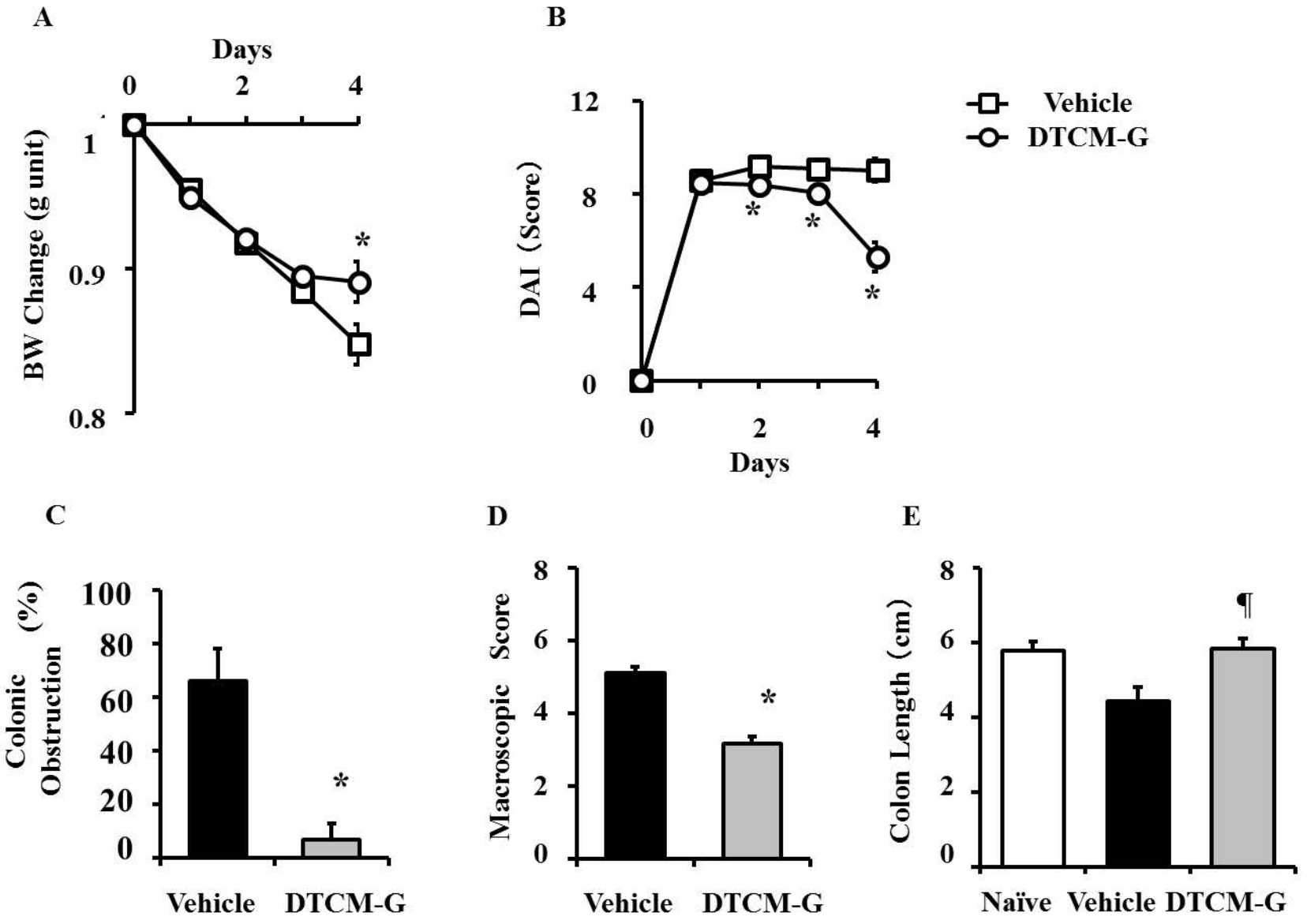
A
Days
0
2
4
1
0.9
0.8
BW Change (g unit)
*
B
12
8
4
0
DAI (Score)
*
*
*
0
2
4
Days
Vehicle
DTCM-G
C
100
80
60
40
20
0
Colonic Obstruction (%)
*
Vehicle
DTCM-G
D
8
6
4
2
0
Macroscopic Score
*
Vehicle
DTCM-G
E
8
6
4
2
0
Colon Length (cm)
¶
Naïve
Vehicle
DTCM-G

Fig 1

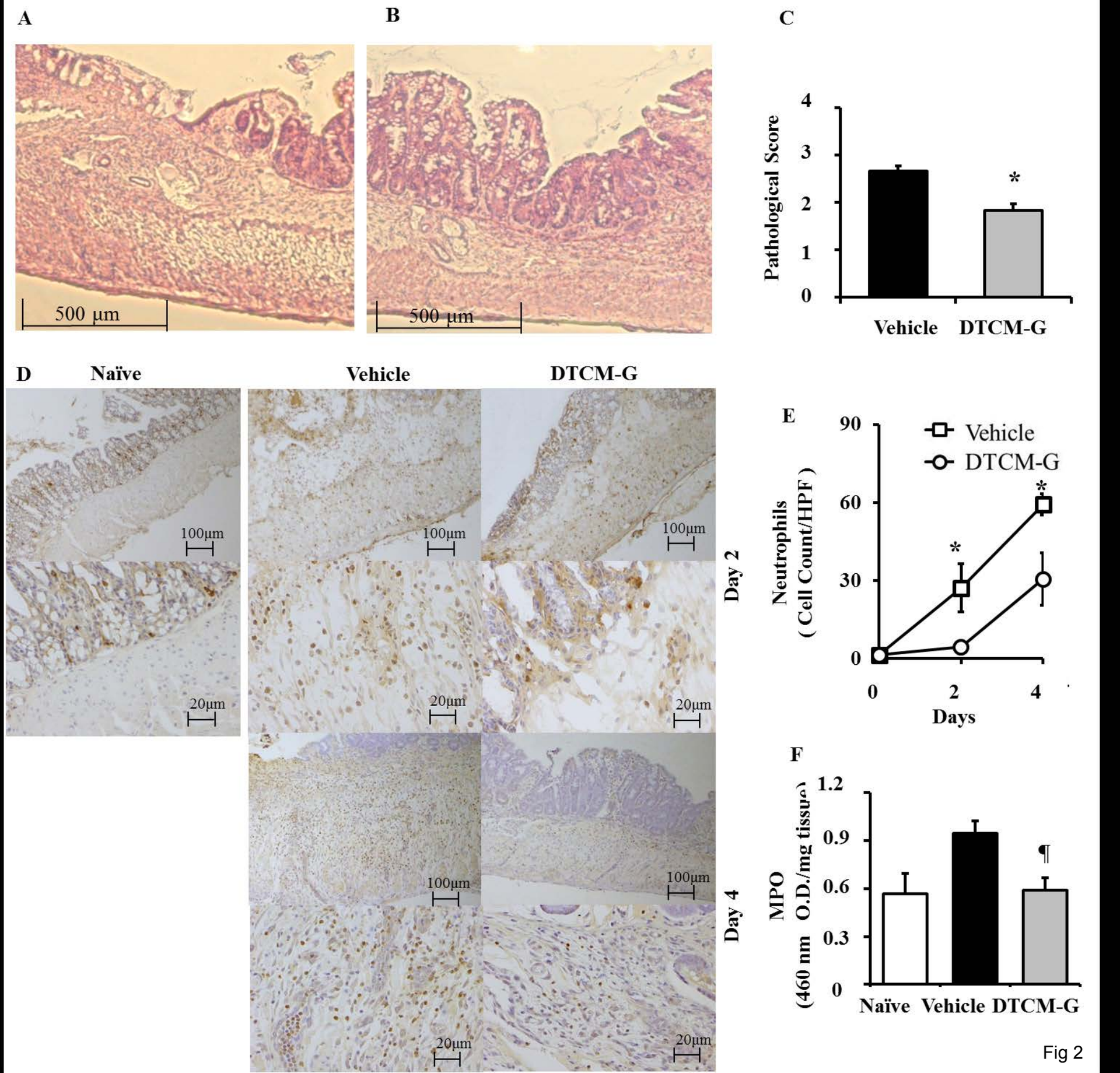
A
B
C
500 μm
500 μm
Pathological Score
4
3
2
1
0
*
Vehicle
DTCM-G
D
Naïve
Vehicle
DTCM-G
100μm
20μm
Day 2
Day 4
E
Neutrophils
(Cell Count/HPF)
90
60
30
0
Vehicle
DTCM-G
*
*
0
2
4
Days
F
MPO
(460 nm O.D./mg tissue)
1.2
0.9
0.6
0.3
0
¶
Naïve
Vehicle
DTCM-G

Fig 2

A

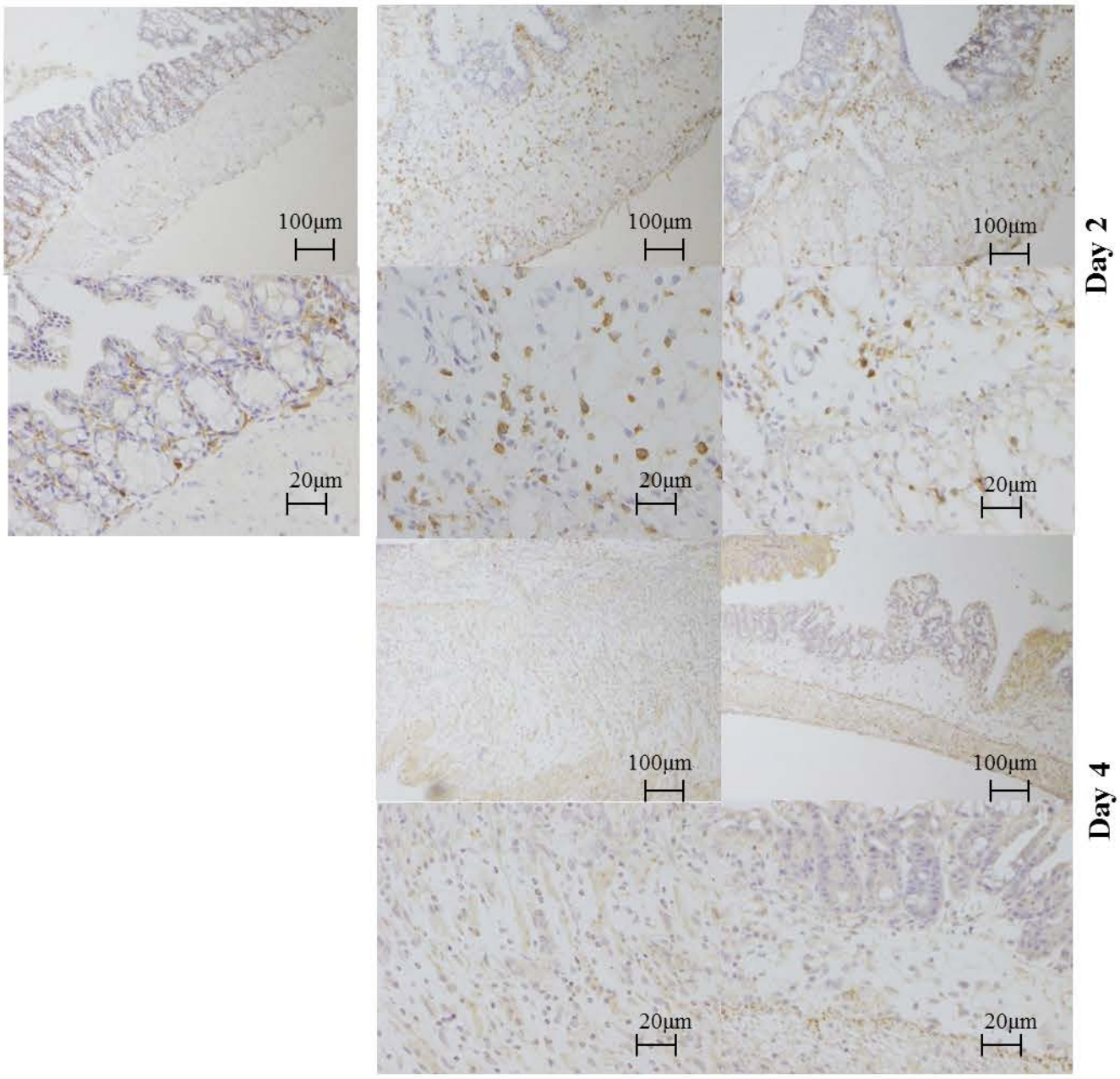
Naïve
Vehicle
DTCM-G
Day 2
Day 4
100μm
20μm

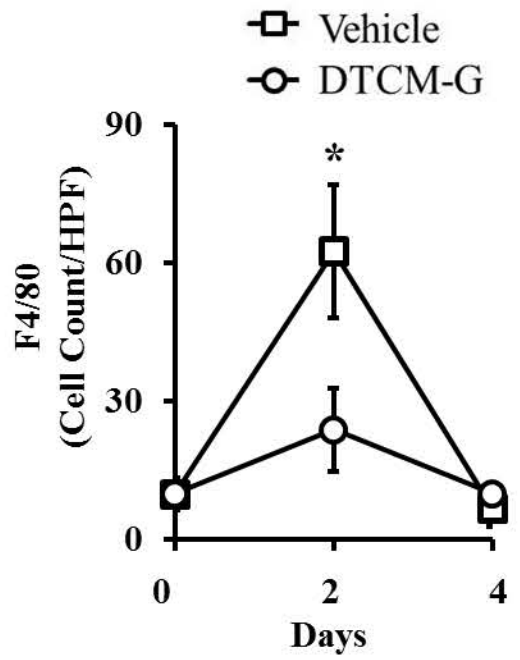
Vehicle
DTCM-G
F4/80
(Cell Count/HPF)
90
60
30
0
*
0
2
4
Days

B

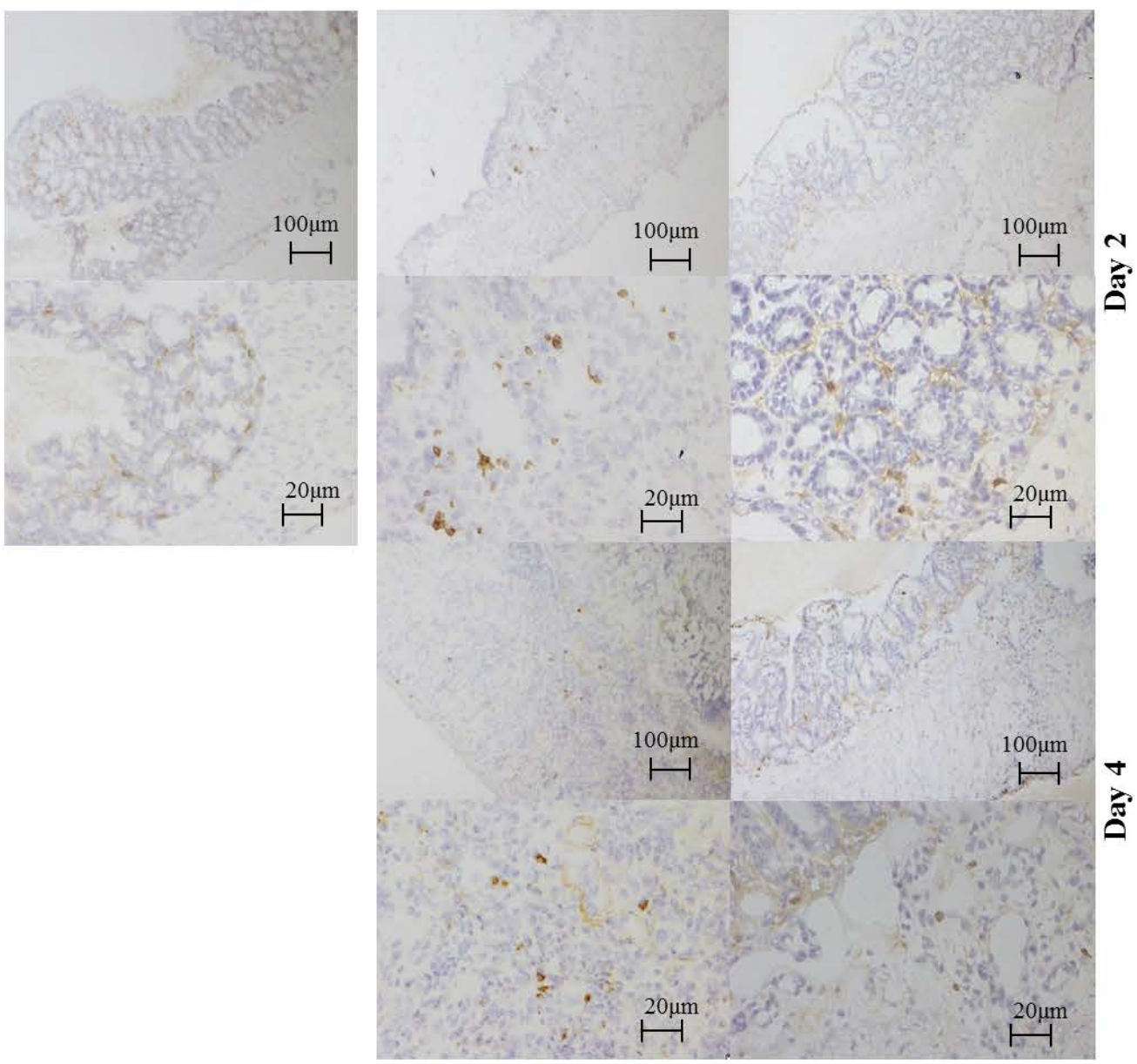
Naïve
Vehicle
DTCM-G
Day 2
Day 4
100μm
20μm

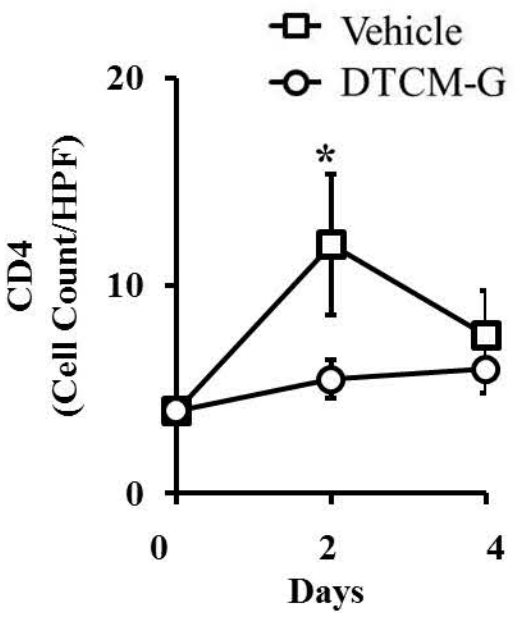
Vehicle
DTCM-G
CD4
(Cell Count/HPF)
20
10
0
*
0
2
4
Days

Fig 3-1

C

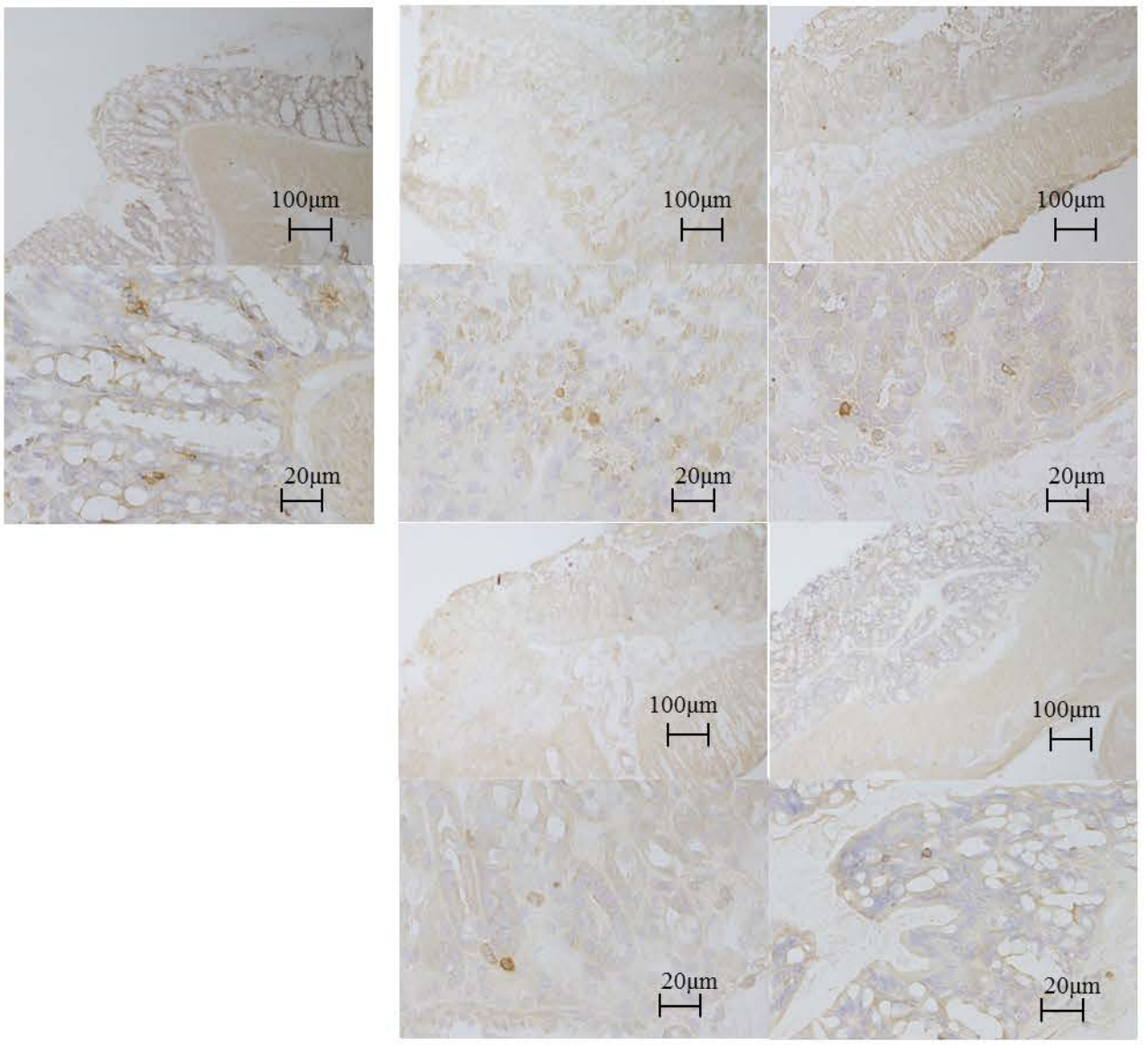

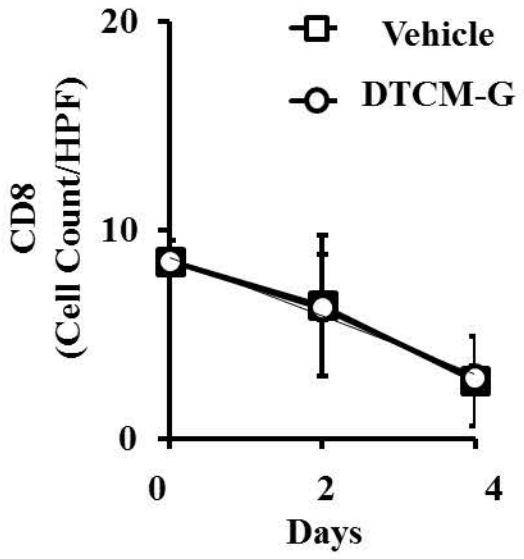

D

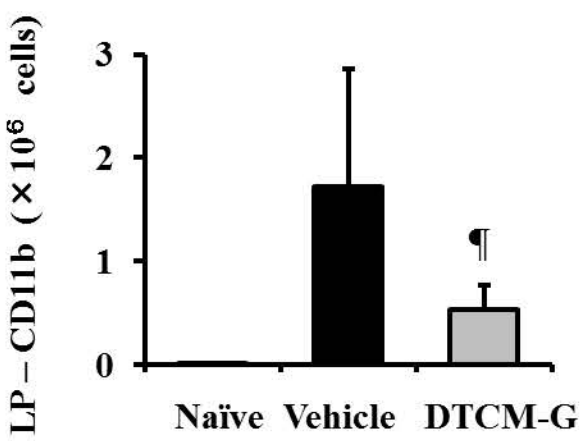

E

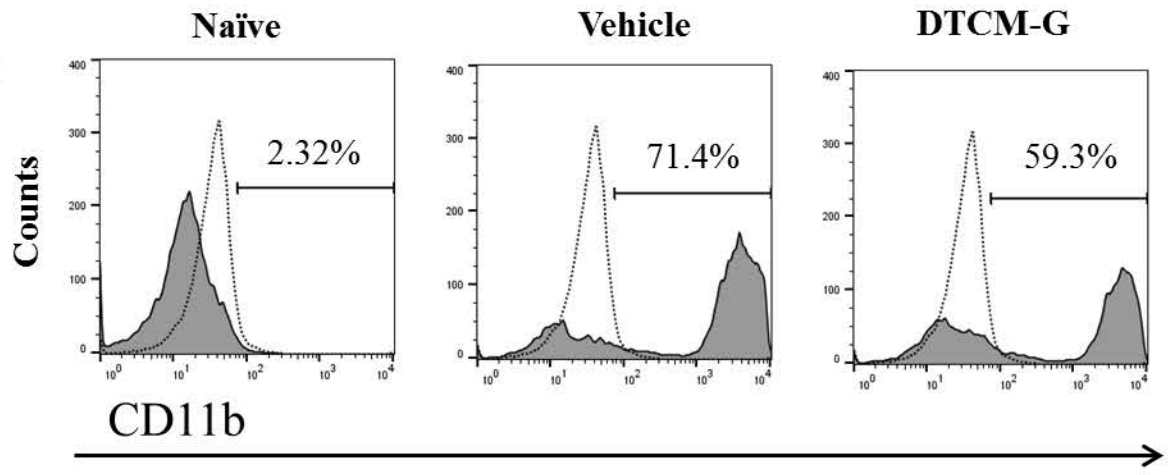

F

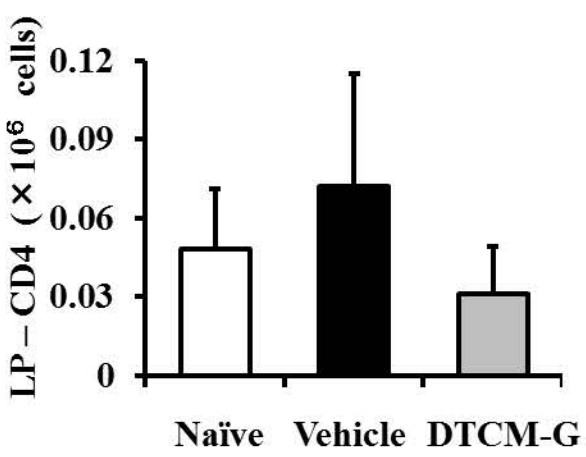

G

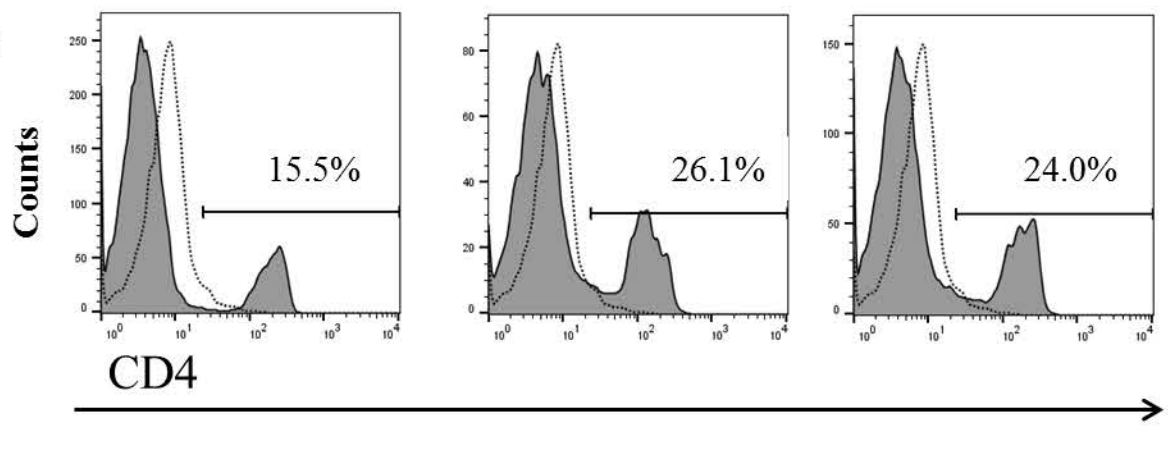

H

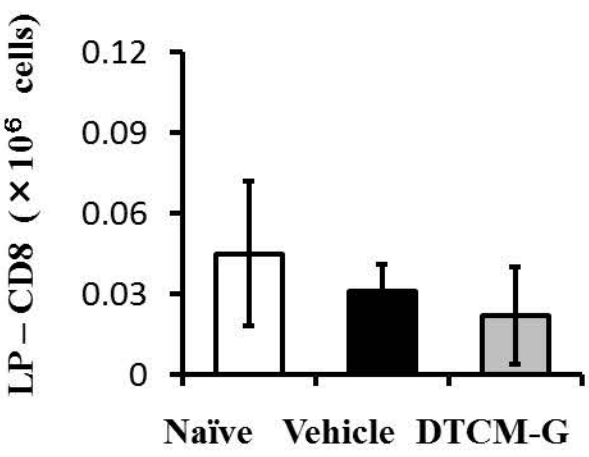

I

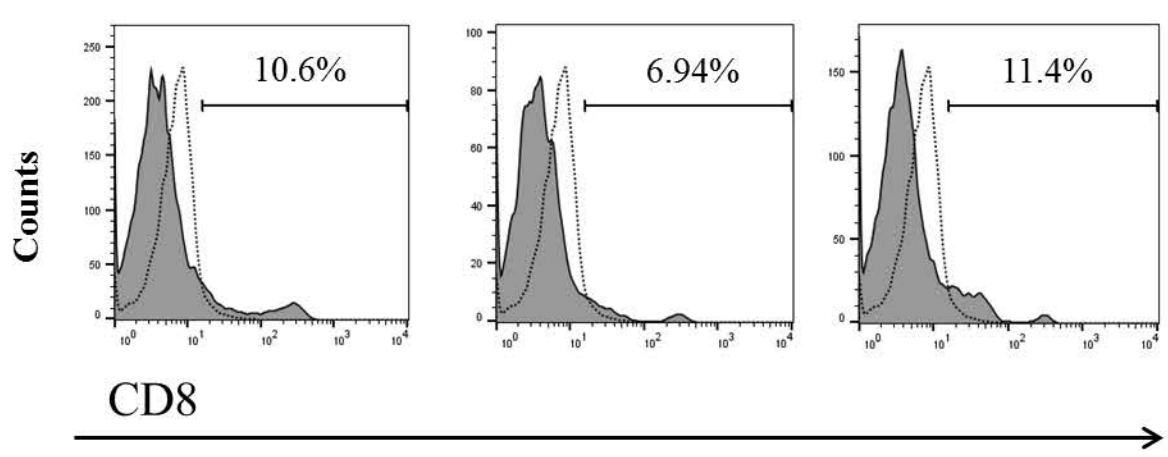

Fig 3-2

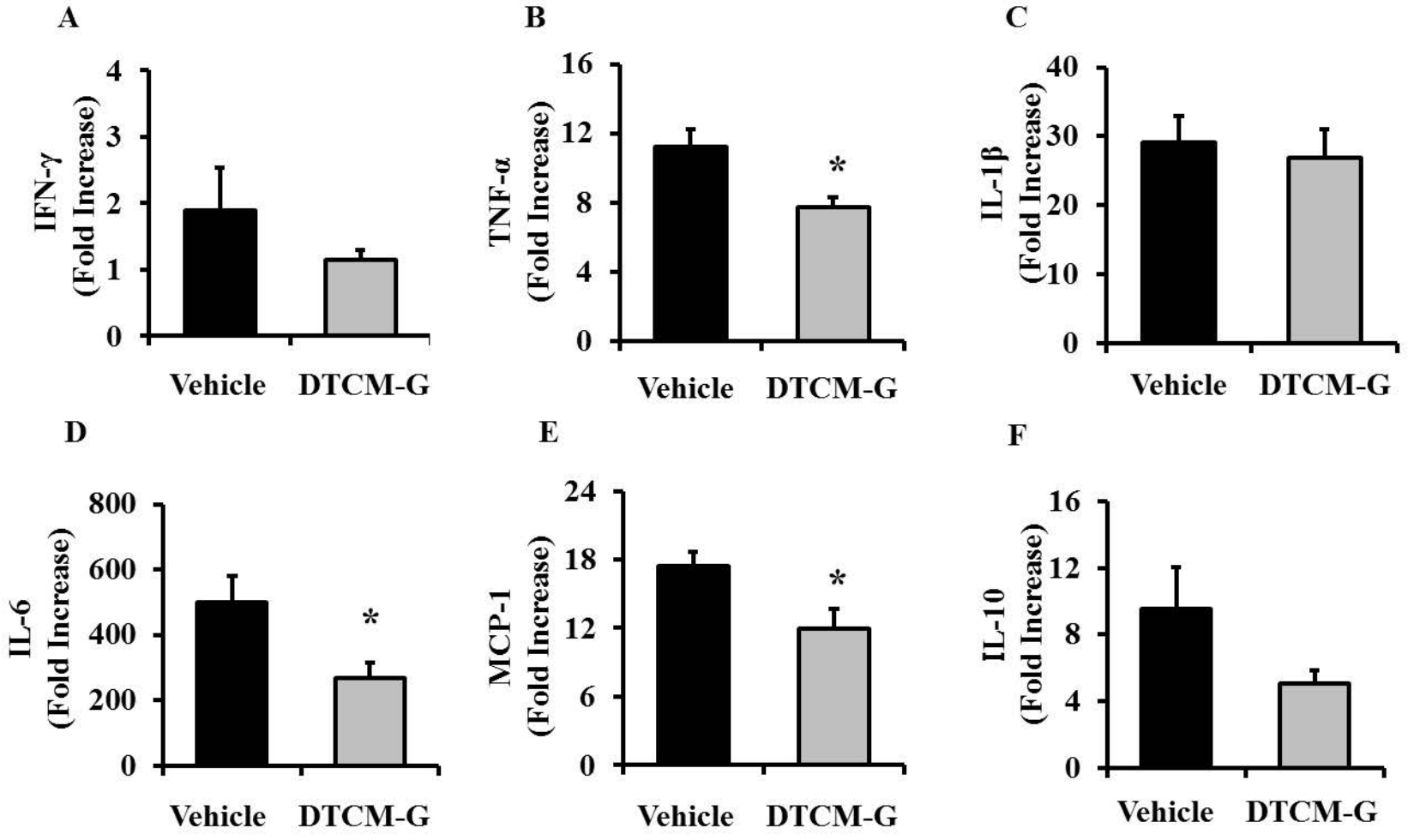
A
IFN-γ (Fold Increase)
0
1
2
3
4
Vehicle
DTCM-G
B
TNF-α (Fold Increase)
0
4
8
12
16
*
Vehicle
DTCM-G
C
IL-1β (Fold Increase)
0
10
20
30
40
Vehicle
DTCM-G
D
IL-6 (Fold Increase)
0
200
400
600
800
*
Vehicle
DTCM-G
E
MCP-1 (Fold Increase)
0
6
12
18
24
*
Vehicle
DTCM-G
F
IL-10 (Fold Increase)
0
4
8
12
16
Vehicle
DTCM-G

Fig 4

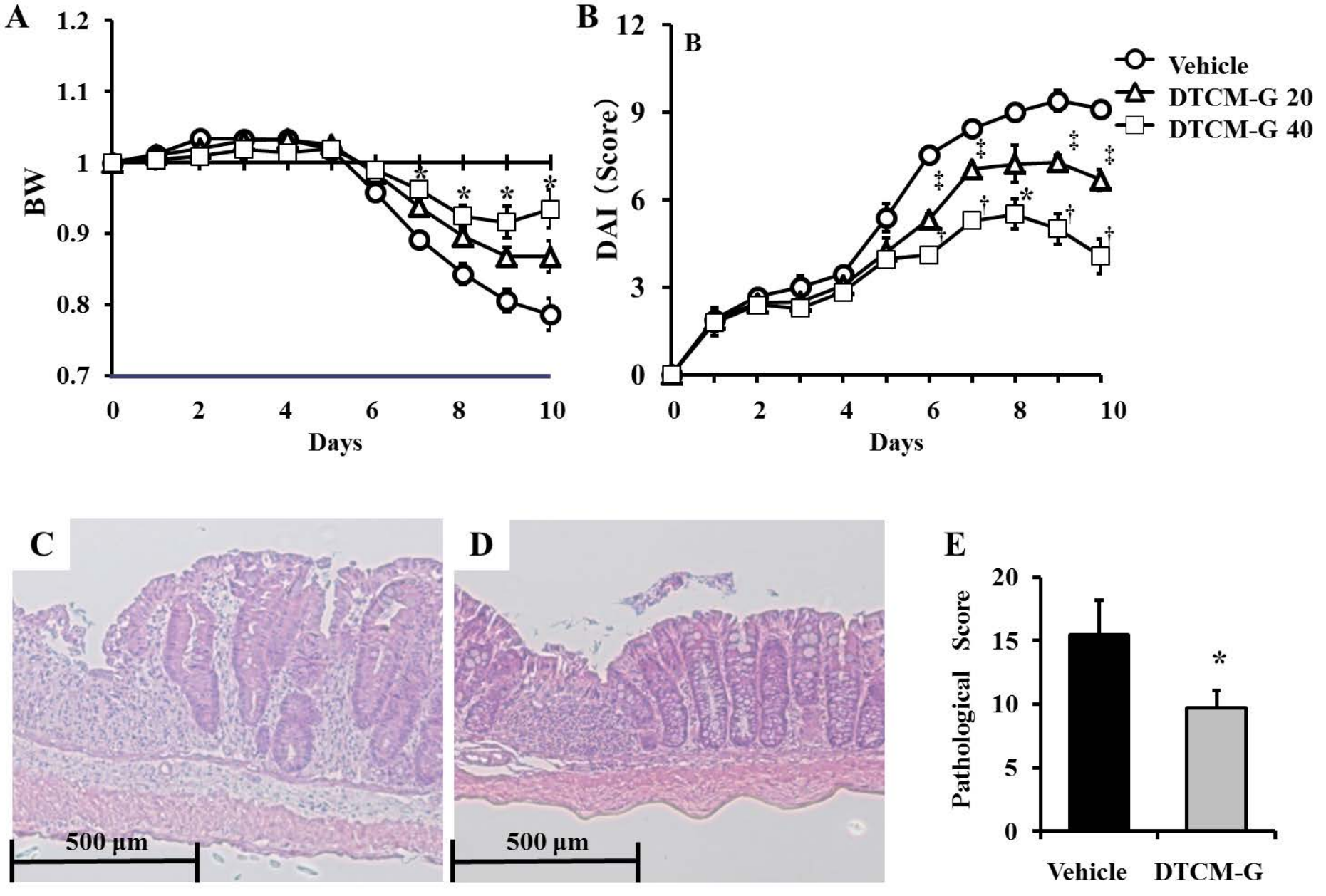
A
1.2
1.1
1
0.9
0.8
0.7
BW
0
2
4
6
8
10
Days
B
12
9
6
3
0
DAI (Score)
Vehicle
DTCM-G 20
DTCM-G 40
C
500 μm
D
500 μm
E
20
15
10
5
0
Pathological Score
Vehicle
DTCM-G

Fig 5

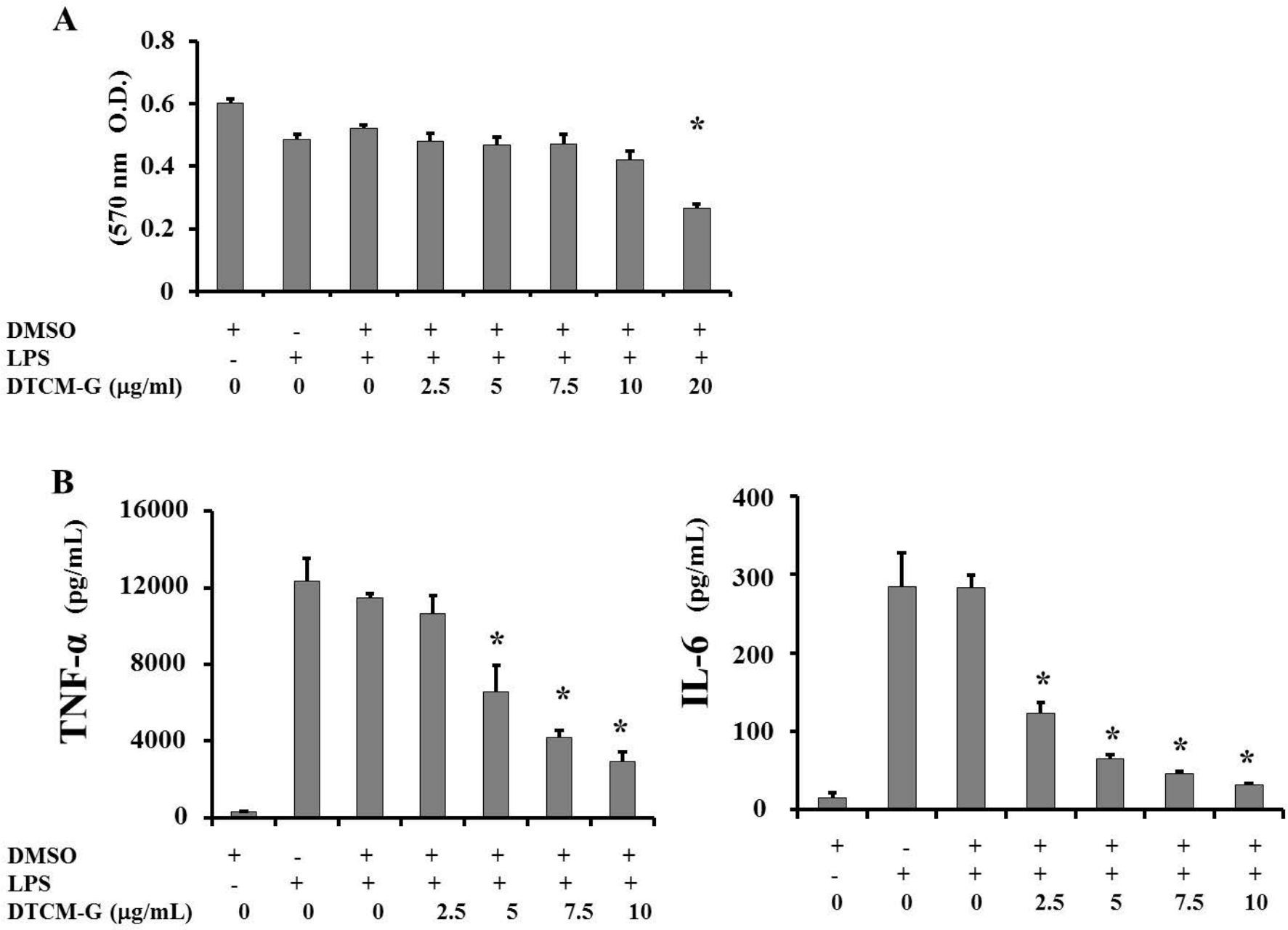
A
(570 nm O.D.)
0.8
0.6
0.4
0.2
0
*
DMSO + - + + + + + +
LPS - + + + + + + +
DTCM-G (μg/ml) 0 0 0 2.5 5 7.5 10 20
B
TNF-α (pg/mL)
16000
12000
8000
4000
0
*
*
*
DMSO + - + + + + +
LPS - + + + + + +
DTCM-G (μg/mL) 0 0 0 2.5 5 7.5 10
IL-6 (pg/mL)
400
300
200
100
0
*
*
*
*
+ - + + + + +
- + + + + + +
0 0 0 2.5 5 7.5 10

Fig 6

A

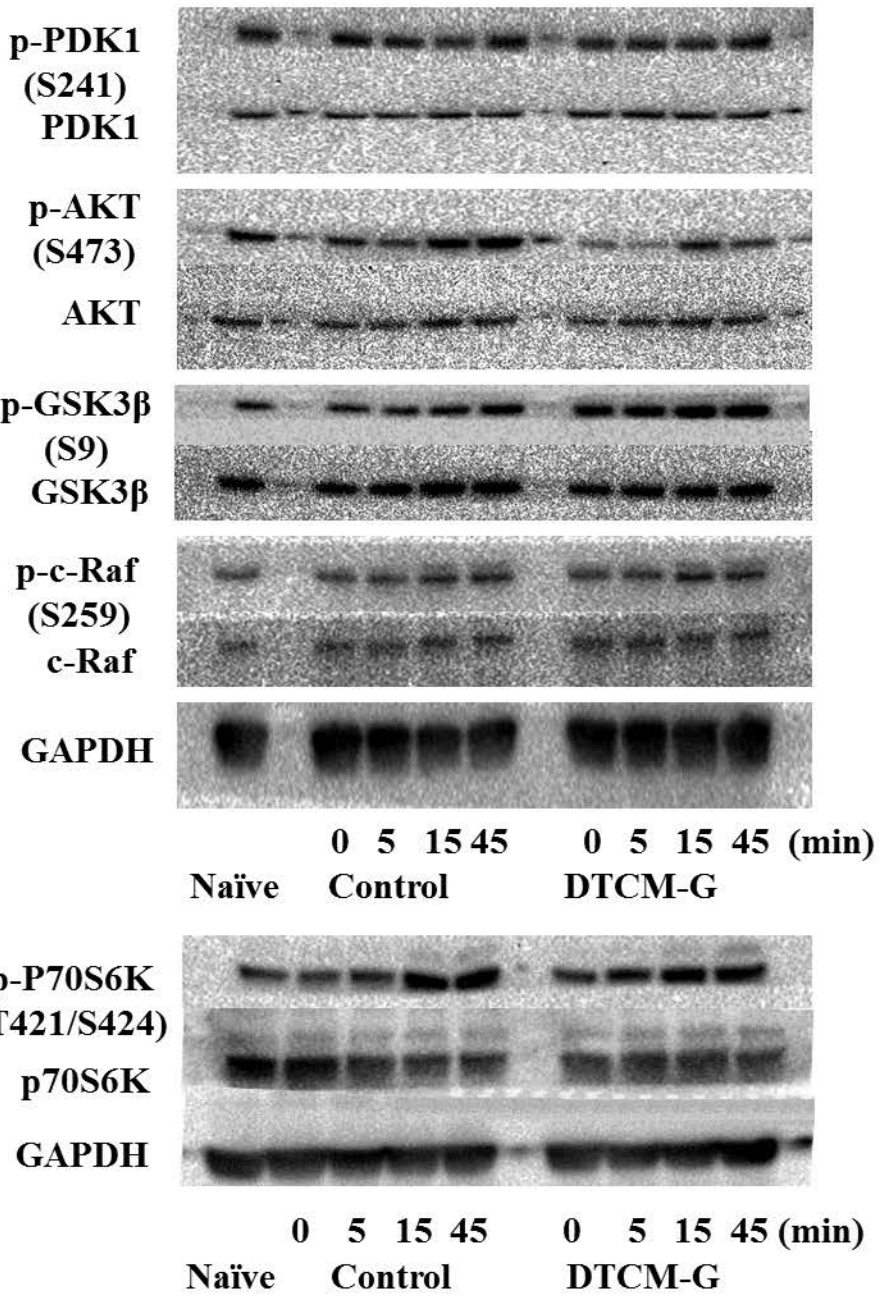
p-PDK1
(S241)
PDK1
p-AKT
(S473)
AKT
p-GSK3β
(S9)
GSK3β
p-c-Raf
(S259)
c-Raf
GAPDH
0 5 15 45 0 5 15 45 (min)
Naïve Control DTCM-G
p-P70S6K
(T421/S424)
p70S6K
GAPDH
0 5 15 45 0 5 15 45 (min)
Naïve Control DTCM-G

B

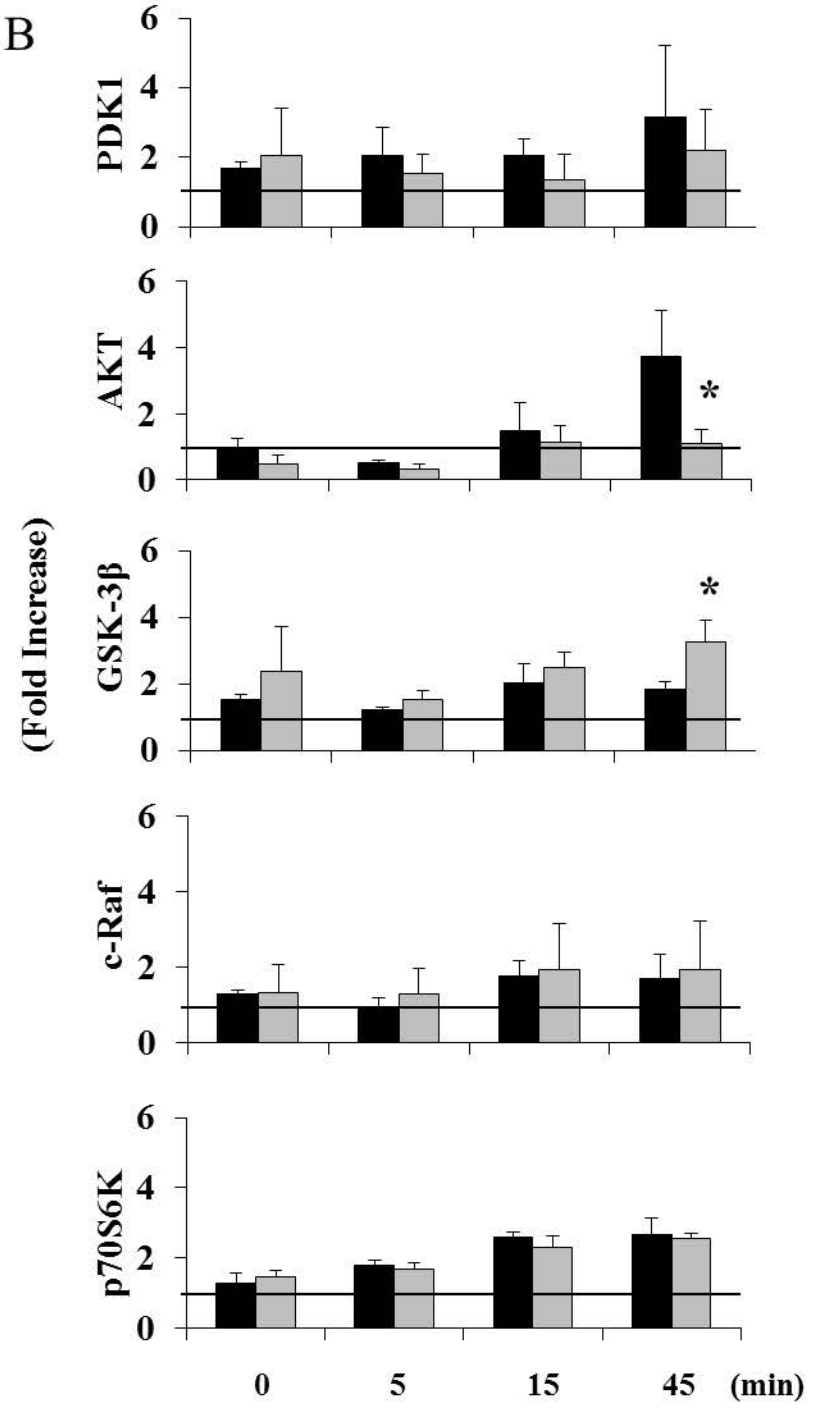
(Fold Increase)
PDK1
AKT
GSK-3β
c-Raf
p70S6K
0
2
4
6
*
0 5 15 45 (min)

C

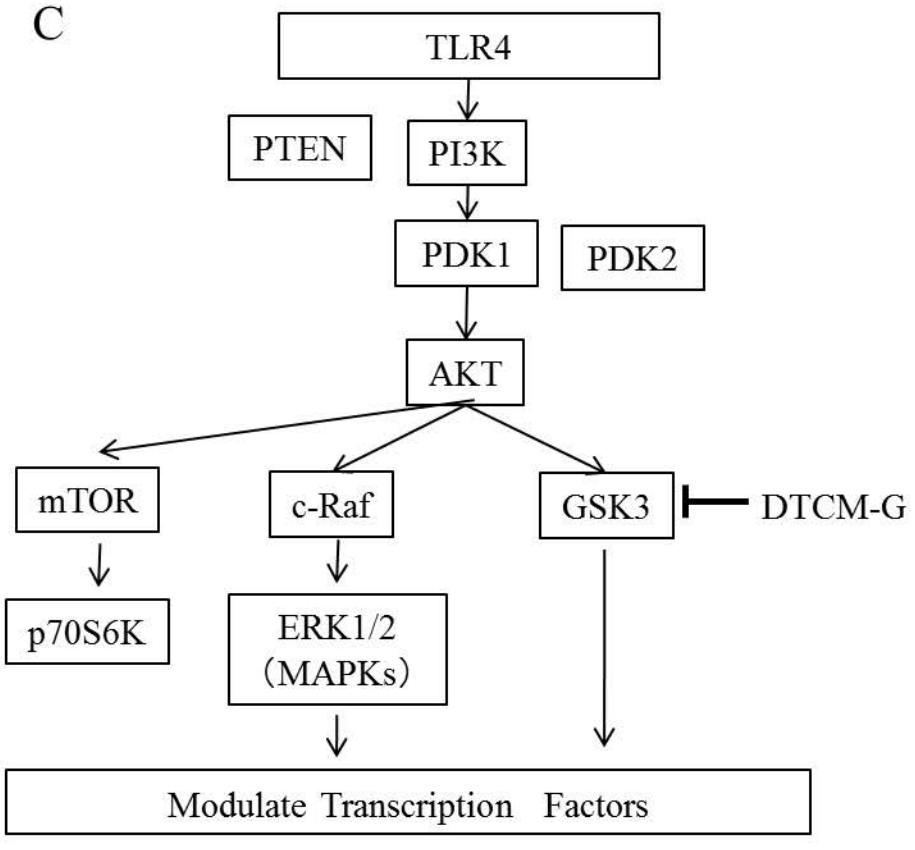
TLR4
PTEN
PI3K
PDK1
PDK2
AKT
mTOR
c-Raf
GSK3
DTCM-G
p70S6K
ERK1/2
(MAPKs)
Modulate Transcription Factors

Fig 7